Metabolic adaptations of pancreatic cancer to a nutrient-deprived environment

A dissertation presented

by

Pei-Yun Tsai

to

The Committee on Higher Degrees in Biological Science in Public Health

In partial fulfillment of the requirements

for the degree of

Doctor of Philosophy

in the subject of

Biological Science in Public Health

Harvard University

Cambridge, Massachusetts

April 2019

Dissertation Advisor: Dr. Nada Kalaany Pei-Yun Tsai

Metabolic adaptations of pancreatic cancer to a nutrient-deprived environment

Abstract

Pancreatic ductal adenocarcinoma (PDAC) is the most common types of the pancreatic cancer, and it is notoriously deadly because the tumor usually is not diagnosed until it's advanced. Several metabolic rewiring mechanisms have been revealed as a hallmark of pancreatic cancer due to its flexibility to acquire nutrient sources through pathways like autophagy and macropinocytosis from the microenvironment. PDAC resides in a unique environment where the tumors are largely occupied by the dense stroma and other types of cell types, which might result in limited nutrient availability.

To understand how PDAC cells manage to overcome limited-glucose and -glutamine conditions, I derived cells that can adapt and proliferate under a prolonged low glucose-low glutamine (L-L) media (these cells are described as adapted cells), and found that they are more tumorigenic *in vivo*. Mechanistically, I demonstrated that the adapted cells can synthesize glutamine from other amino acids sources, such as leucine or glutamate with elevation in glutamine synthetase (GS) protein expression. In addition, adapted cells maintain the activity of mechanistic target of rapamycin complex 1 (mTORC1) under the L-L conditions. Apart from some of the well-known regulations underneath mTORC1 signaling, I demonstrated that mTORC1 activity can also stabilize GS protein, which might further reinforce the glutamine synthesis ability of adapted cells.

To better understand if glutamine synthesis is present *in vivo* and in patients, I showed that PDAC can synthesize glutamine in an *ex vivo* setting by ^{15}N-tracer, and GS protein is expressed in

various degrees in PDAC patients. In addition, genetic and pharmacological approaches to inhibit GS suppressed cell proliferation under nutrient-poor conditions. These results highlight the possibility that GS can be a potential therapeutic target in PDAC.

Table of Contents

List of Figures

Figure 3.10. The heatmap and a pathway illustration of genes upregulated in adapted clones within fatty acid degradation pathway compared to non-adapted clones under L-L conditions.

Acknowledgements

There are countless people that I would like to thank during my graduate school study. First, I would like to thank Dr. Nada Kalaany for always being enthusiastic and supportive in guiding my project over the past few years. I would like to thank our former and current lab members (Clare, Tamara, Ashley, Peter, and MinSik) for all the help either in the lab or things in life. I would like to thank MinSik and Peter joined my thesis project toward the end of my thesis, so my project was able to progress much faster. Thank you all for bringing so much laughter in the lab. I would especially want to thank Clare for being my great friend, not only in the lab but also outside of the lab. We had so much fun memories that made my life in graduate school unforgettable.

I would like to thank Dr. Bob Farese, Dr. Alex Toker, and Dr. Marcia Haigis for providing me many great advices during my DAC meetings. Thank you all for always taking time for me and offering me helps whenever I needed. I would like to thank Dr. David Christiani, Dr. Jean Zhao, and Dr. Dohoon Kim for taking the time to serve as my defense committee.

I would like to thank my country, Taiwan, for providing me the fellowship to come to the US, so I could have a memorable experience here. I would like to thank many faculties and staff in the BPH program (Dr. Marianne Wessling-Resnick, Dr. Brendan Manning, Dr. Tun-Hou Lee, Deirdre, Tom), and thank all the committees who gave me the offer six years ago. I would like to thank my classmate Vanessa Byles, who is so clever in science and always being a supportive friend.

I would like to thank my friends here, including Oliver Stoehr, Margaret Liao, and Yenee Soh. Thank you all for always being there for me and listening to my ups and downs. My life will be much more stressful without you.

Lastly, I would like to thank Tsai family, my dad, mom, and sister. Without you, I probably cannot make it to the end of graduate school. I would like to thank you all from the bottom of my heart. Thank you, mom! Thank you for praying for me every day.

I would not have been this closed to get a PhD without countless people who have influenced me throughout the years. So, I want to thank all of them.

Chapter 1: Introduction

1.1 Metabolic alterations in pancreatic cancer

1.1.1 Overview

Pancreatic ductal adenocarcinoma (PDAC), which accounts for 90% of pancreatic cancer, has a 5-year survival rate of only 9%. This disease is predicted to be the second leading cause of cancer-related death in the United States within the next decade (*1*). There are several factors that account for the low survival rate, including a late onset of disease presentation (*2, 3*), a unique tumor microenvironment (*4-6*), and distinct cellular metabolic or genomic alterations (*7, 8*). The majority of PDAC patients experience metastasis by the time of death. This aggressive behavior of PDAC is a cause of its resistance to conventional therapy. Cytotoxic chemotherapeutic agents are the only approved treatments for these patients. However, they only show a minimum effect to extend patients' survival. Therefore, researchers are still trying to discover new effective drugs and also to find biomarkers for early detection.

Gain-of-function mutations in KRAS at codons 12, 13 are commonly found in > 90% of the PDA patients (*9*). KRAS mutation, along with loss-of-function mutations in three specific tumor suppressor genes (TP53, CDKN2A, and SMAD4), lead to the progression from a benign tumor to a carcinoma (*10*). KRAS encodes a small GTPase protein, which shuttles between the active guanosine triphosphate-bound (GTP) state and the inactive guanosine diphosphate-bound (GDP) state (*11*). Oncogenic substitution at codon G12 or G13 inhibits the interaction with the GTPase activating protein (GAPs), which promotes KRAS-GTP binding and leads to constitutive activation of downstream signaling pathways, such as Mitogen-activated protein kinases (MAPK) and PI3K/AKT/mTOR pathways (*12*).

Oncogenic KRAS-driven signaling can promote tumorigenesis by rewiring canonical metabolic pathways. In order to meet the demands for cellular proliferation and growth, cancer

cells must have efficient ways to produce building blocks, to generate energy, and to have the ability to encounter environmental stress.

1.1.2 The microenvironment of pancreatic cancer

PDAC has a unique microenvironment characterized by hypovascularization, leading to a high interstitial fluid pressure with a reduced drug efficacy (*4*). PDAC exhibits a more hypoxic and nutrient-deprived microenvironment when compared to the surrounding benign tissue (*13*), resulting in alternative nutrient acquisition pathways that I will discuss later. A heterogenous mixture of different types of cells and extracellular matrix (ECM) reside within tumors (*14*). Among these, the stellate cells, which are specialized fibroblasts called cancer associated fibroblast (CAF), are present as the major cell type in the PDAC tumor microenvironment and account for ECM production (*15*). Other cell types include tumor-associated macrophages (TAMs), immune cells (T cells, B cells), endothelial cell, and neurons.

Due to the heterogeneity of the tumor microenvironment, many reports demonstrated that there are intra-tumoral metabolic cross-talks between different types of cells (*14*). For example, hypoxic cancer cells utilize glucose for anaerobic glycolysis and secrete lactate as the end product through monocarboxylate transporter (MCT1). On the other hand, lactate can be consumed and further metabolized to the tricarboxylic acid (TCA) cycle and can fuel oxidative phosphorylation in well-oxygenated cancer cells in the PDAC model (*16*). This demonstrates that PDAC cells are able to recycle "waste" –in this case, lactate –and utilize it as a nutrient source to promote tumorigenesis.

Besides the glucose-lactate shuttle observed in PDAC tumors, pancreatic cancer CAFs have also been shown to secrete the amino acid alanine to fuel the TCA cycle in PDAC cancer

cells, and to further support fatty acids and non-essential amino acid (NEAA) biosynthesis (*17*). Interestingly, the authors also demonstrated that the alanine-derived carbon can compete with the glucose- and glutamine-derived carbon. The presence of CAFs enhanced tumor growth *in vivo*, indicating that targeting both cancer cells as well as other cell types that present in the microenvironment such as CAFs might be a better approach for targeting PDAC growth.

Several other reports showed that the presence of adipocytes residing in obese PDAC patients might lead to poor survival (*18*). In an *in vitro* study (*19*), pre-adipocytes could support PDAC cell proliferation under glucose- and glutamine-starved conditions, mirroring the harsh conditions *in vivo.* This indicates that there is a nutrient-shuttling between pancreatic cancer cells and adipocytes.

Recently, Halbrook *et al.* (*20*) showed that TAM-released deoxycytidine could compete with the conventional chemotherapy drug- gemcitabine, leading to the resistance to gemcitabine in PDAC cells. Furthermore, depleting myeloid cells in mouse model sensitized PDAC tumors to gemcitabine treatment. This finding shows a novel role of cross-talk between macrophage and cancer cells. Interestingly, although they identified several pyrimidine metabolites being secreted from alternatively activated macrophages, it remains to be uncovered what the physiological function of the pyrimidine exchange is.

1.1.3 Metabolic rewiring in pancreatic cancer

In order to support anabolic growth and proliferation under nutrient-depleted conditions, cancer cells have adapted by rewiring their metabolism in many ways. Unlike normal cells, cancer cells present higher glycolytic rates and secrete lactate in the presence of oxygen, which was originally attributed to defective mitochondria and impaired aerobic respiration; however,

subsequent work has shown that mitochondrial function is not impaired in most cancer cells. The alteration of metabolic processes is further considered as one of the hallmarks of cancer (*21*).

Often times, the alteration of metabolism is induced or suppressed by oncogenic mutations (*22-24*). Oncogenic KRAS-driven signaling can promote tumorigenesis by rewiring canonical metabolic pathways (Fig. 1.1). For example, previous studies have shown that KRAS activation promotes glucose uptake by increasing glucose transporter-GLUL1 expression and enhancing glycolytic flux through enhanced gene expression (*Gpi1, Pfkl, Pfkm, AldoA, Tpi1*, *HK1*, and *HK2*) in the glycolysis pathway (*22, 25*). $Kras^{G12D}$ was also shown to induce the hexosamine biosynthesis pathway (HBP), with increases the generation of glucosamine-6-phosphate (GlcN-6P) important for protein modification. Moreover, $Kras^{G12D}$ activates the non-oxidative branch of pentose phosphate pathway (PPP) to promote ribose biosynthesis (*25*).

Although most of cells utilize the oxidative-arm of PPP to generate NAPDH, which is important to prevent oxidative stress, PDAC utilizes glutamine in a non-canonical way, whereby glutamine-derived aspartate is transported to into the cytoplasm, where it is then converted to oxaloacetate by aspartate transaminase (GOT1). The oxaloacetate is subsequently converted into malate and then pyruvate, generating NADPH as a by-product. The increased $NADPH/NADP^+$ ratio can maintain the cellular redox state in PDAC (*26*). Activation of KRAS signaling not only regulates glucose and glutamine metabolism, but also regulates nutrient acquisition pathways, such as autophagy and macropinocytosis (*27*) (Fig. 1.2).

Macroautophagy (referred to as autophagy hereafter) is a conserved catabolic process in eukaryotes that results in the degradation of intracellular organelles, unfolded proteins, or cytoplasmic material in the lysosome to provide building blocks such as amino acids, fatty acids, or nucleotides during cellular stress or starvation conditions (*28*). One of the well-known regulator

of autophagy is the mechanistic target of rapamycin (mTOR), which is a serine-threonine protein kinase that forms two functionally and biochemically distinct complexes, mTOR complex 1 (mTORC1) and mTOR complex 2 (mTORC2) that I will discuss later. Under nutrient-replete conditions, mTORC1 suppresses autophagy through phosphorylation of a protein complex composed of unc-51-like kinase 1 (ULK1), autophagy-related gene 13 (ATG13), and focal adhesion kinase family-interacting protein of 200 kDa (FIP200), which are required to initiate autophagy (*29-31*). In contrast, nutrient deprivation stimulates the ULK1/ATG13/FIP200 complex formation and initiates autophagy through ULK1 auto-phosphorylation and phosphorylation of its binding partners (*29-31*). Another important regulator of autophagy is 5'-AMP-activated protein kinase (AMPK), which is induced upon energy starvation. Under low nutrient supply, such as glucose starvation, the ratio of (AMP+ADP)/ATP increases, leading to the activation of AMPK, which in turn binds to and activates ULK1 through direct phosphorylation at Ser317, Ser777, and Ser555 in murine proteins (*32, 33*).

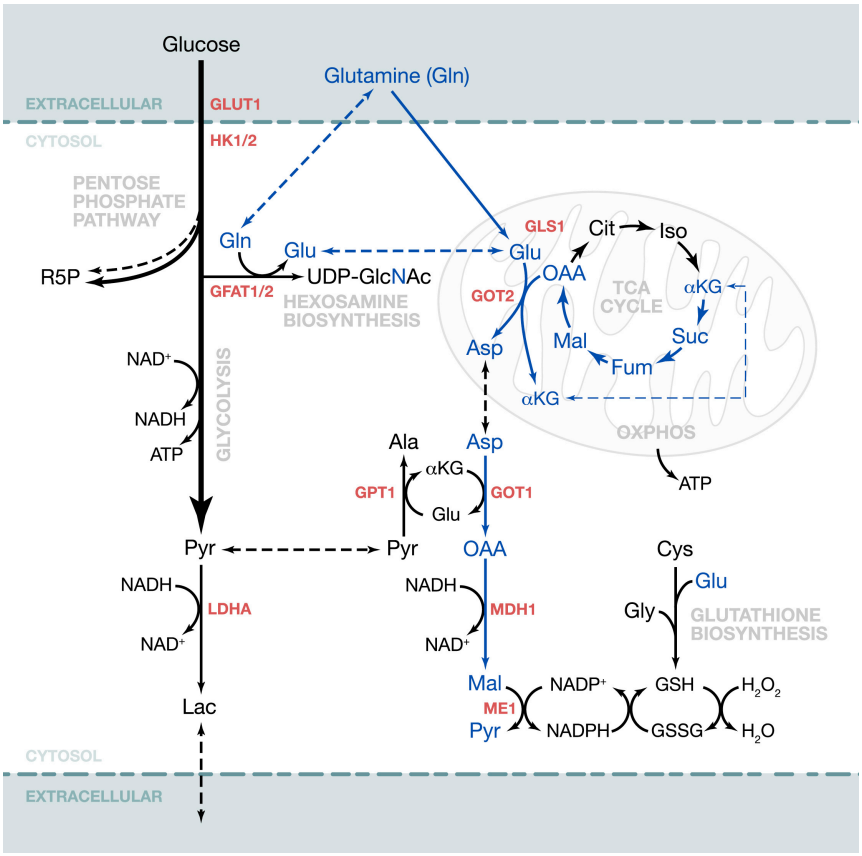

Figure 1.1. Metabolic alterations in PDAC

Oncogenic Kras enhances glucose transporter GLUT1 expression and activates expression of some glycolytic enzymes, resulting in the elevation of glycolytic flux. Glucose also serves as an important carbon source for anabolic metabolism by shunting the carbon to the pentose phosphate pathway (PPP) and the hexosamine biosynthetic pathway. PDAC cells rely on a KRAS-rewired glutamine (Gln) metabolic pathway for redox balance, where Gln is converted to glutamate (Glu) through GLS1 then aspartate (Asp) through GOT1 in the mitochondria. Aspartate further shuttles to the cytosol and generate NADPH through a series of reactions. This maintains the reduced glutathione (GSH) levels, which is important for redox homeostasis. Blue indicates that the metabolites and metabolic pathways are utilizing carbon from Gln.

Figure reprinted from Christopher J. Halbrook and Costas A. Lyssiotis, Cancer cell, 2017.

PDAC, however, has been shown to maintain high levels of basal, even in nutrient-replete conditions (*34*). It has been shown that the transcription factor MiT/TFE, which regulates autophagy by binding to a DNA element involved in the expression of multiple autophagy and lysosomal genes, is activated in PDA independent of mTOR signaling (*35*). In order to understand the role of autophagy in tumor initiation and progression, researchers have been using genetically engineered mouse models (GEMMSs) that harbor deletions in essential autophagy genes. In general, it has been shown that autophagy suppresses tumor initiation by reducing reactive oxygen species (ROS) through the removal of damaged organelles. However, once tumors have been established, activation of autophagy can provide the fuels (amino acids, fatty acids, and nucleotides) for tumor progression (*36, 37*). In line with this, conditional ablation of autophagy gene- ATG5 or ATG7 in GEMMs showed attenuation of tumor growth (*36, 37*). Similarly, pharmacological treatment with hydroxychloroquine (HCQ), which inhibits lysosomal acidification, reduces tumor volume in mice bearing established tumors (*36, 37*).

Beside the cell-autonomous role of autophagy in promoting cancer progression, a recent report showed that an autophagy-dependent crosstalk between stroma and tumor cells is also important for tumor progression. Stellate cells, or the most abundant fibroblasts in PDA microenvironment, can secrete alanine through an autophagy-dependent pathway for its use by the surrounding cancer cells. This suggests that in a nutrient-deprived environment, tumor cells can use alternative nutrient sources provided by other cell types within the TME, to fuel anabolism (*17*), as I have mentioned earlier. Overall, this indicates that inhibiting autophagy in both cancer cells and the stroma might be beneficial for patient survival. However, there remains a need for a specific autophagy inhibitor to be used in the clinic.

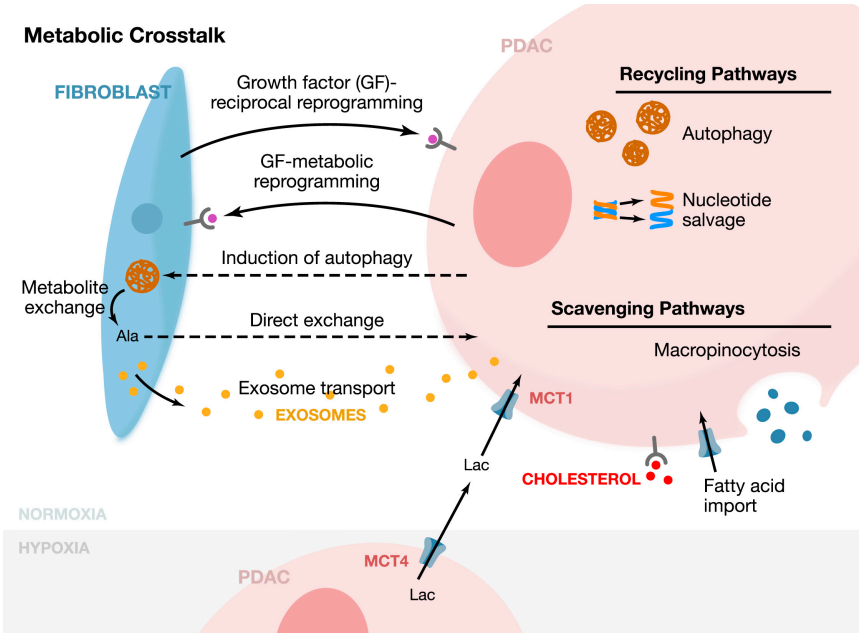

Figure 1.2. Nutrient acquisition pathways in PDAC

Pancreatic cancer cells are involved in multiple metabolic crosstalks with stromal cells. Growth factors released from PDAC cells can metabolically reprogram fibroblasts, which reciprocally respond to epithelial cells. PDAC cells can induce autophagy in pancreatic stellate cells, which then release alanine (Ala) to promote PDAC cell growth. Metabolite exchange also occurs in cancer cells, as PDAC cells in hypoxic environments release lactate (Lac), which fuels proliferation in normoxic cancer cells. Pancreatic cancer cells are capable of recycling nutrients and macropinocytic scavenging of extracellular macromolecules, such as proteins and lipids, to maintain nutrient levels in a starved tumor microenvironment.

Figure reprinted from Christopher J. Halbrook and Costas A. Lyssiotis, Cancer cell, 2017.

.

Another nutrient acquisition pathway that PDAC depends on is macropinocytosis. While autophagy can supply nutrients to the cancer cells, it cannot create a net increase in biomass, due to self-degradation. Whereas macropinocytosis is also a lysosome-dependent pathway, it can engulf extracellular fluid containing proteins and lipids, which get further degraded in the lysosome to supply fuels. Activation of macropinocytosis can be regulated by oncogenic *RAS* (*38*). In PDAC, cells can uptake exogenous protein through macropinocytosis to supply central carbon metabolites during glutamine-starvation conditions. This effect is abrogated by a known macropinocytosis inhibitor- 5-[N-ethyl-N-isopropyl] amiloride (EIPA) (*38*). Both *ex vivo* and *in vivo* reports have shown that exogenous proteins contribute to the amino acid pool in PDAC tumors (*38, 39*). Taken together, macropinocytosis serves as a mean to increase biomass by scavenging exogenous sources during tumor proliferation could be a possible target to attenuate PDAC growth.

1.2 The microenvironment modulates the tumor metabolic phenotype

1.2.1 Overview

Emerging studies have shown that although cancer cells consume glucose rapidly and the increased glycolytic flux can be used to generate intermediate macromolecules, environmental nutrient conditions can impact the cancer cells' flexibility to utilize different nutrients or to metabolize nutrients in different ways. One of the hurdles to understand cancer metabolism is the discrepancy between nutrient levels *in vitro* and *in vivo*. Lactate, a metabolite usually considered a waste from glycolysis, has proven to serve as a carbon source for the TCA cycle in mice bearing human non-small cell lung cancers (NSCLC) (*40*). In another NSCLC murine model, a tracing

experiment showed that glutamine has only a small contribution to the TCA cycle; instead, oxidation of glucose plays a major role in supplying carbons to the TCA cycle *in vivo* (*41*). While cell culture media provide sufficient nutrients *in vitro*, solid tumors are usually exposed to harsh conditions, such as hypoxia and nutrient depletion in the microenvironment. To survive under these harsh conditions, cancer cells reprogram their metabolism in response to different kind of stress. Under hypoxic conditions, or 0.1 – 2% compared to 5% normal oxygen tension, the transcription factor-hypoxia-inducible factor HIF1-alpha is stabilized and activates genes involved in glycolysis, including the glucose transporters (GLUT)- GLUT1 and GLUT3 (*42*). This, in return, promotes glucose uptake and enhances the glycolytic flux; HIF-1α also down-regulates oxidative phosphorylation by phosphorylating pyruvate dehydrogenase kinase 1 (PDK1) (*43*). PDK1 phosphorylates and inactivates pyruvate dehydrogenase (PDH), thereby inhibiting the conversion of pyruvate to acetyl-CoA in entering the TCA cycle. Besides its regulation of glycolysis, HIF-1α has also been shown to regulate lipid synthesis in several ways, including enhanced expression of *FASN* and *LPIN1*, which are required for fatty acid synthesis (*44, 45*).

In recent years, a few groups have been trying to understand how cancer cells rewire their metabolism in culture media containing nutrient levels similar to physiological human plasma. Cantor *et al.* showed that the high levels of uric acid present in the Human Plasma-Like Medium (HPLM) inhibit *de novo* pyrimidine synthesis by directly inhibiting uridine monophosphate synthase. This then desensitizes cancer cells to the chemotherapeutic agent 5-fluorouracil (5-FU) (*46*). On the other hand, Voorde *et al*. demonstrated that by growing cancer cells in Plasmax, which contains around 60 nutrients and chemicals at the same concentrations as those found in human blood, profoundly influences metabolism when compared to commercial DMEM medium (*47*). For instance, the supraphysiological concentrations of pyruvate in DMEM can

stabilize hypoxia-inducible factor 1α (HIF1 α) in normoxia, therefore inducing a pseudohypoxic transcriptional program. In addition, the high levels of arginine in DMEM can reverse the urea cycle reaction catalyzed by argininosuccinate lyase (ASL), which has not been observed *in vivo*, and is prevented by Plasmax *in vitro*. These results might explain why researchers have been struggling to translate the results from basic into clinical research to cure cancer.

Since two-dimensional (2D) culture does not recapitulate all the features of tissues *in vivo*, including extracellular matrix, stiffness, and nutrients (metabolite and oxygen) gradients, many groups have developed three-dimensional (3D) organoid culture systems that more closely mimic *in vivo* genotype, phenotype, and functions with an *in vitro* system (*48-50*). By generating an organoid from patient-derived primary tissues and supplemented with Matrigel or basement membrane extract as ECM substitutes in specific culture medium (*51*), researchers have been attempting to assess drug efficacy (*52*), drug toxicity (*53, 54*), or even harnessing this technology for personalized medicine (*55*).

Although a 3D culture system is a better way to mimic *in vivo* tumor growth, it is still not a perfect model, given the complexity and heterogeneity in tumors. Therefore, optimizing it or finding other tools in the future would benefit our understanding of cancer biology.

1.2.2 Reprogramming of glucose and glutamine metabolism in cancer

In the past decade, there has been a growing interest among researchers in cancer metabolism, primarily with regard to glucose metabolism. The aerobic glycolysis phenomenon, also known as the Warburg effect, was first addressed by the German scientist Otto Warburg in the 1920s (*56, 57*), Warburg also made the assumption that oxidative phosphorylation (OXPHOS) is impaired in cancer cells (*58*), although this was later challenged by many who showed that most

tumors maintain intact OXPHOS (*59, 60*). The distinction between cancer cells and normal cells lead to the application of FDG-PET imaging in patients since tumor cells are avid for glucose (*61*). Glucose is the main nutrient for tumor growth as it plays an important role not only in glycolysis, but also in several other processes (*62*). The glucose-derived carbon is involved in: a- the pentose phosphate pathway (either oxidative or non-oxidative), which generates nucleotides and NADPH, which is required for fatty acid synthesis and can be scavenged by reactive oxygen species (ROS) (*63*); b- the hexosamine biosynthesis pathway, which involves glycosylation of proteins (*64*); c- the serine-glycine and the one-carbon pathway, which is important for integrating carbon for amino acids, lipids, nucleotide synthesis, and for maintaining redox levels. This pathway is also involved in methylation processes, which is important for epigenetic regulation (*65*).

Although glucose is the most important nutrient for cancer survival, high demand of glucose by tumor cells can lead to exhaustion of glucose supply in solid tumors (*66, 67*). For example, the average glucose concentrations in the tumors from stomach cancer and colon cancer were detected at 0.1mM and 0.4 mM, respectively, in contrast to the average blood glucose concentration of 6 mM (*68*). Due to this phenomenon, several reports investigated how cancer cells adapt to glucose starvation. Birsoy *et al*. exposed 28 patient-derived cancer cell lines in a continuous flow culture apparatus (Nutrostat) to low glucose (0.75 mM) media, and found that cells with impaired OXPHOS function or with mtDNA mutations in Complex I genes are sensitive to glucose starvation, suggesting that cells with intact OXPHOS function would be able to survive under glucose-limiting conditions (*69*). In another report, Huang *et al.* showed that lactate rescues glucose starvation-induced cell death in NSCLC by activating the PI3K/Akt/mTOR pathway (*70*).

Glutamine, on the other hand, is the most abundant amino acid in the plasma. It not only provides a carbon source for replenishing the TCA cycle through glutamine anaplerosis, but also

provides a nitrogen source for amino acid, nucleotide, and hexoamine synthesis. Glutamine-derived glutamate is also involved in glutathione biosynthesis, which is required for redox homeostasis (*71*). Many cancer cells including PDAC cells or oncogene-transformed cells are dependent on glutamine, and cannot survive without exogenous glutamine (*26, 72-74*). Once cells uptake glutamine through their transporters, glutamine can be converted to glutamate and ammonia through glutaminases (GLS 1 or GLS2). While GLS1 is overexpressed in several cancer cells, GLS2 is less well understood (*75*). Inhibition of GLS with genetic or pharmacological approaches has been shown to impede tumor growth in several studies that I will discuss later. Glutamate can then be converted to alpha-ketoglutarate (αKG) in 2 different ways: 1- via glutamate dehydrogenases (GLUD), either GLUD1 or GLUD2, to produce ammonia and αKG; and 2- via aminotransferases, so that the amino group of glutamate becomes part of non-essential amino acids, including alanine, aspartate and serine. This transamination reaction includes alanine aminotransferase enzymes (cytosolic GPT1 and mitochondrial GPT2), which catalyze the reversible reaction of the amino group transfer from glutamate to pyruvate to produce α-KG and alanine; aspartate aminotransferase (cytosolic GOT1 and mitochondrial GOT2), which catalyze the reversible reaction of the amino group transfer from glutamate to oxaloacetate to produce α-KG and aspartate; and lastly, phosphoserine aminotransferase (PSAT), which catalyzes the reversible reaction of the amino group transfer from glutamate to 3-phosphohydroxypyruvate to produce α-KG and phosphoserine.

The most well-known mutations driving glutamine dependency in cancer cells include the oncogenes KRAS and MYC, as well as the tumor suppressor p53. Oncogenic KRAS alters glutamine metabolism by making it dependent on transaminases and it can further generate

NADPH for balancing redox status, as I mentioned previously (*26*). MYC coordinates the gene expression that regulates glutamine metabolism at the transcriptional and post-transcriptional levels (*76*). For example, MYC transcriptionally represses miR-23a/b, leading to higher expression of mitochondrial GLS. p53 induces GLS2 expression, which displays an opposite function of GLS1 in tumorigenesis, as p53 is considered to be a tumor suppressor (*77*).

Besides upregulation of glutaminase, some cancer cells can also synthesize glutamine through the glutamine synthetase (GS) enzyme, also termed glutamate-ammonia ligase (GLUL), when the cells are under glutamine starvation. Under physiological conditions, GS is important for nitrogen metabolism due to assimilation of ammonia and glutamate for glutamine synthesis. It is highly expressed in perivenous hepatocytes that surround the central veins, and its main role is to detoxify ammonia in liver (*78*). In addition, GS is important in the brain since it converts the neurotransmitter L-glutamate into L-glutamine (*79*). GS is also highly expressed in some cancers. For example, Tardito *et al.* showed that the enhanced GS activity under glutamine starvation fuels *de novo* nucleotide synthesis in glioblastoma (*80*). Bott *et al.* demonstrated that overexpression of c-MYC oncogene increases GS expression through promoter demethylation in breast cancer cell lines, and the elevated expression of GS can promote cell survival under glutamine limitation (*81*). Hepatocellular carcinoma also presents high GS expression (*82, 83*). Different cancer subtypes can show distinct patterns of glutamine metabolism, even with cells derived from the same organ. For instance, luminal breast cancers frequently exhibit high GLUL and low GLS expression, whereas basal breast cancers have low GLUL and high GLS (*84*). In addition to cancer, cancer-associated fibroblasts (CAF) up-regulate GS and glutamine synthesis, which provides a glutamine source for surrounding ovarian cancer cells growth *in vivo (85)*.

Regulation of GS varies depending on cancer types, cell types, and locations. For example, expression of GS is tightly regulated by β-catenin in perivenous hepatocytes (*86*) and hepatocellular carcinoma cell lines (*87*). GS expression is known to be a sensitive indicator of nutrient deprivation as its expression level is under the control of the starvation-sensing transcription factor forkhead box O3a (FOXO3A) (*88*). MYC oncogene can regulate GS transcriptionally or post-transcriptionally (*76, 81*). Nguyen et al. demonstrated that high glutamine availability can regulate GS at post-translational level by degrading it in the proteasome (*89*).

1.2.3 Targeting glutamine metabolism as a therapeutic approach in cancer

Given that cancers in different tissues rely on exogenous glutamine for amino acid and nucleotide synthesis, and glutamine is important for TCA cycle anaplerosis, suppression of glutamine metabolism became an attractive strategy for cancer therapy. Gamma-l-glutamyl-p-nitroanilide (GPNA), the inhibitor of the glutamine transporter SLC1A5, has been shown to effectively suppress tumor growth in NSCLC xenografts (*90*).

Small molecule inhibitors, such as bis-2-(5-phenylacetamido-1,2,4-thiadiazol-2-yl)ethyl sulfide (BPTES) or CB-839 from the Calithera company, represent a new class of metabolism-targeting drugs that inhibit GLS isoforms given that glutaminase activity is induced in many cancers, including breast (*91*), pancreatic (*26*), and colorectal cancers (*92*). Although BPTES can suppress many types of cancers *in vitro* and *in vivo*, it is not a good candidate for GLS inhibition due to its poor solubility. CB839 in currently being testing in clinical trials along with other inhibitors to treat patients with renal cell carcinoma, breast cancer, or colorectal cancer that bear mutations in PIK3CA or KRAS (Calithera company website).

Although CB-839 showed good efficacy in many cancers, it has only been demonstrated to suppress pancreatic cancer growth *in vitro* but not *in vivo*. Biancur *et al.* showed that pancreatic cancer cells can adapt to glutaminase suppression, by inducing an anti-oxidant response and fatty acid metabolism (*93*), highlighting the importance of administering a combination therapy along with glutaminase inhibitors.

1.3 The multifaceted role of mTORC1

1.3.1 Overview

The mechanistic target of rapamycin (mTOR) is an evolutionarily conserved serine/threonine protein kinase that acquire its name due to the discovery of an immunosuppressant drug-Rapamycin, which was originally identified as an antifungal drug (*94*). Rapamycin forms a complex with peptidyl-prolyl-isomerase FKBP12 to inhibit down-stream effectors of mTOR signaling (*95, 96*).

mTOR signaling is commonly activated in tumors, which is activated by genetic alterations (*97, 98*) or nutrient inputs (*99*). It plays an important role for orchestrating the integration of nutrients and anabolic responses, which are critical for cancer metabolism and tumor growth. Therefore, it is important to understand the roles and functions of this master regulator.

1.3.2 Regulation of metabolism by mTORC1

mTOR exists in two distinct complexes, known as mTOR Complex 1 (mTORC1) and mTOR Complex 2 (mTORC2). mTORC1 includes three core components: mTOR, Raptor (regulatory protein associated with mTOR), and mLST8 (mammalian lethal with Sec13 protein 8)

(*100, 101*), whereas mTORC2 contains mTOR, mLST8 and Rictor (rapamycin insensitive companion of mTOR). mTORC1 signaling has been more extensively studied than mTORC2. Herein, I will focus on discussing the downstream network of mTORC1 signaling.

mTORC1 plays an important role in balancing between anabolic and catabolic responses (Fig. 3). Among anabolic processes, mTORC1 promotes proteins, lipid, and nucleotides synthesis in order to support cell growth and proliferation. On the other hand, mTORC1 suppresses catabolic processes, such as autophagy and protein degradation. I will discuss these in the greater detail.

mTORC1 induction of protein synthesis is its best characterized by downstream effect pathways involve in mTORC1 signaling. mTORC1 stimulates mRNA translation by directly phosphorylating its downstream substrates. For example, mTORC1 phosphorylates the eukaryotic translation initiation factor (eIF4E)-binding protein 1 and 2 (4E-BP), thus interrupting the interaction with eIF4E. This then recruits eIF4G, forming an initiation complex at the 7-methyl-GTP cap of the mRNA and promoting mRNA translation (*102*). mTORC1 also phosphorylates ribosomal protein S6 Kinase 1 and 2 (S6K 1/2), which promote translation by phosphorylating downstream translation factors (*103*).

Cancer cells have a high demand for nucleotides during proliferation. The nucleotide pool within cells can come from either *de novo* synthesis or the salvage pathway through

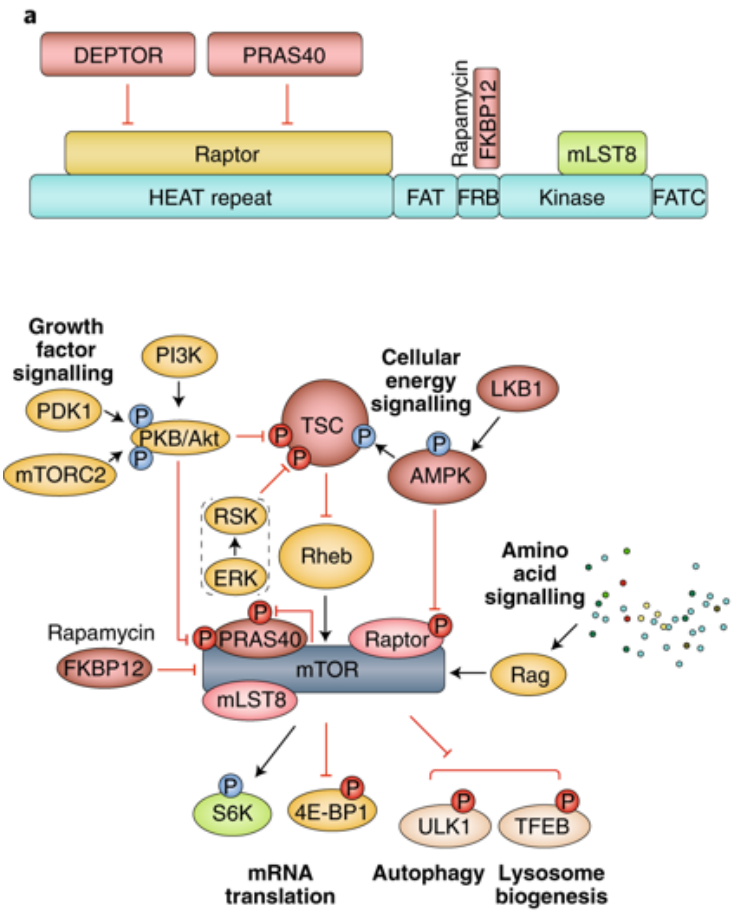

Figure 3. Molecular composition and upstream regulators of mTORC1

The upper panel shows the schematic representation of mTORC1 subunits and the mTOR domain structure. mTORC1 contains mTOR, Raptor, mLST8, PRAS40, and DEPTOR. mTOR is composed of huntingtin-elongation factor 3-regulatory subunit A of PP2A-TOR1 (HEAT) repeat, FRAP–ATM–TTRAP (FAT), FRB, kinase (catalytic domain) and FAT domain at C terminus (FATC). The binding sites of mTORC1 subunits on mTOR are also shown. In the lower panel, key players in mTORC1 signaling are shown, including upstream regulators that integrate growth factor and cellular energy signaling into mTORC1. The major downstream effectors that mediated by mTORC1 are mRNA translation, autophagy and lysosomal biogenesis.

The figure is reprinted from Joungmok Kim and Kun-Liang Guan, Nature Cell Biology, 2019.

recycling pre-existing intermediates in nucleotide metabolism (*104*). Composing purine and pyrimidine rings requires amino acids and ribose-5-phophoribosyl-1-pyrophosphate (PRPP) generated by the pentose phosphate pathway (PPP). mTORC1 signaling has been shown to activate the PPP pathway by different mechanisms (*105, 106*). Synthesis of purine metabolism requires glutamine, aspartate, glycine, formyl-tetrahydrofolate (fTHF), CO2, and inosine monophosphate (IMP), which is derived from PRPP. mTORC1 regulates purine synthesis through transcription factors, such as Myc, sterol regulatory element binding protein (SREBP), and activating transcription factor 4 (ATF4), all of which enhance this process (*107*). On the other hand, pyrimidine synthesis requires glutamine, aspartate, bicarbonate (HCO_3^-), and PRPP. mTORC1 regulates pyrimidine synthesis pathway by phosphorylating the trifunctional enzyme carbomoyl phosphate synthetase 2, aspartate transcarbamylase and dihydroorotate (CAD), which is the rate-limiting enzyme in pyrimidine synthesis pathway. mTORC1 regulates *de novo* pyrimidine synthesis through phosphorylation of the CAD enzyme by its downstream effector S6K. The phosphorylated CAD then oligomerizes to promote pyrimidine synthesis (*108, 109*). Highly proliferating cells, such as cancer cells, require not only nucleotides for rRNA and DNA synthesis, but also lipid synthesis for membrane generation and signaling. mTORC1 activates SREBP1, the main transcription factor that induces lipogenic genes, such as ATP citrate lyase (ACLY), acetyl-CoA carboxylase 1 (ACC1), fatty acid synthase (FASN), and stearoyl-CoA desaturase 1 (SCD1) (*110-112*).

While mTORC1 stimulates these anabolic processes, it also inhibits catabolic processes, such as autophagy. mTORC1 is reported to directly phosphorylate and suppress ULK1, the kinase complex required to initiate autophagy, as I have discussed above (*29*). In addition, mTORC1 can

directly phosphorylate and inhibit the transcription factor TFEB, which controls many genes with key roles in lysosomal function (*113, 114*).

effectors that mediate mTORC1 effects on mRNA translation, autophagy and lysosomal biogenesis

mTORC1 also suppresses macropinocytosis, a process involving the endocytic uptake of extracellular proteins that are then degraded in the lysosome. Inhibition of mTORC1 was reported to support cell survival in tumors residing in a poorly vascularized and highly nutrient-depleted environment, such as pancreatic cancer (*115*).

Two major quality-control pathways responsible for protein homeostasis are autophagy and the ubiquitin-proteasome system (UPS). In 2014, Zhang *et al.* demonstrated that mTORC1 signaling increases proteasome-mediated protein degradation through induction of the transcription factor –nuclear factor erythroid-derived 2-related factor 1 (NRF2) (*116*) –and the degraded substrates can be used for protein synthesis. However, two more recent reports showed that inhibition of mTORC1 increases rather than decreases the proteasome-dependent proteolysis of long half-life proteins through enhanced ubiquitination in mammalian cells or increased proteasomal regulatory particle assembly-chaperones (RACs) in yeast (*117, 118*).

1.3.3 Nutrients sensing pathways to activate mTORC1

Activation of mTORC1 is well-characterized by the presence of growth factors, amino acids, and energy. However, other mTORC1 activators remain to be explored. Growth factors, including insulin/insulin-like growth factor (IGF-1), trigger PI3K-AKT signaling (*119*). AKT phosphorylates and inhibits TSC1-TSC2 complex (*120, 121*), which causes TSC complex to dissociate from the lysosome, enabling the GTPase protein Rheb to activate mTORC1 (*122, 123*).

Although Rheb is essential for mTORC1 activation, under amino acids starvation, mTORC1 is still not fully activated (*101*). Ras-related GTPase (Rag) protein plays an important role in the amino acid sensing pathway for activating mTORC1 (Fig. 4). Four Rag proteins exist in mammals. RagA and RagB, each of which can form heterodimers with either RagC or RagD. GTP-loaded RagA/B in complex with RagC/D localize to the lysosomal surface and interact with another protein complex termed the Ragulator and an amino acid transporter SLC38A9 (*124, 125*). The role of the Rags is to recruit mTORC1 to lysosomal Rheb, where mTORC1 can be fully activated.

Several cytosolic sensors have been identified that activate mTORC1 signaling. For instance, SLC38A9 is a lysosomal arginine sensor that interacts with the Rag GTPase-Ragulator complex that is necessary for the efflux of leucine and the activation of mTORC1 (*126-128*); Sestrin is a cytosolic leucine sensor by negatively regulates GATOR2, which is upstream of mTORC1. Leucine, when present, binds to sestrin and interrupt the interaction with GATOR2, leading to the inhibition of GATOR1 and further activation of RagA/B and mTORC1 (*129, 130*); CASTOR1 is a cytosolic arginine sensor that can either form a homodimer or a heterodimer with CASTOR2. Binding of arginine to CASTOR relieves the inhibition of CASTOR on GATOR2, thereby activating mTORC1(*131*). More recently, a S-adenosylmethionine (SAM) sensor upstream of mTORC1 (SAMTOR) was identified as another regulator of mTORC1. Increased levels of SAM due to higher levels of methionine result in the binding of SAM to SAMTOR, causing the disruption of SAMTOR-GATOR1 binding, and hence activation of mTORC1 (*132*). Despite the remarkable progress achieved in recent years in our understanding

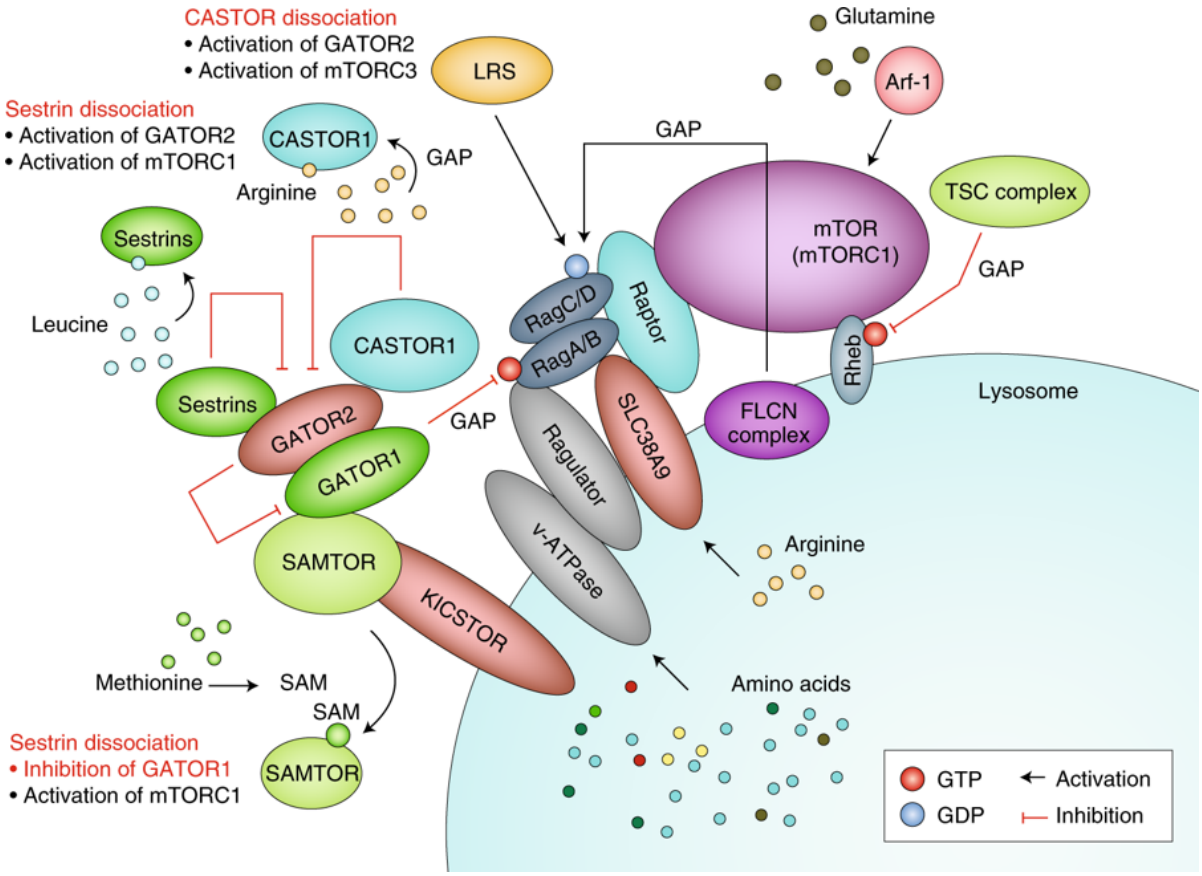

Figure 4. mTORC1 sensors

Sestrins, CASTOR1, and SAMTOR are cytosolic sensors. Sestrins and CASTOR1 sense leucine and arginine, respectively. Upon amino acid binding, they dissociate from GATOR2, releasing their suppressive effects on GATOR2 (the positive regulator of mTORC1) and thus activate mTORC1. SAMTOR senses methionine in the form of SAM. Upon SAM binding, SAMTOR dissociates from and relieves its inhibition on GATOR1 (a negative regulator of mTORC1), thus leading to mTORC1 activation. Arf-1 relays the glutamine signals to mTORC1 activation through a Rag-independent mechanism. SLC38A9 is a lysosomal arginine sensor and is essential for mTORC1 activation by increasing the arginine level in the lysosome.

The figure is reprinted from Joungmok Kim and Kun-Liang Guan, Nature Cell Biology, 2019.

of mTORC1 signaling, many questions remain unsolved regarding the upstream and downstream regulation of mTORC1. Given that it is a master regulator that converges nutrient signals to alter metabolism, deregulation or hyperactivation of mTORC1 has been linked to many human diseases, incuding cancer, obesity, and type-2 diabetes. Therefore, ongoing and future studies investigating the regulation of mTOR complexes would benefit human health.

1.4 Overview of the dissertation

PDAC tumors are known to reside in a nutrient-poor, hypovascularied microenviroment, that is not reflected in standard cell culture media composition. Indeed, several reports recently pointed at discrepancies between *in vitro* and *in vivo* metabolic studies in cancers, including PDAC. These are partly attributed to the use of cell culture media containing supraphysiological levels of nutrients. In this dissertation, I first provide some evidence to show the importance of understanding PDAC metabolism for therapeutic purposes.

In Chapter 2, I derive human PDAC clonal cells that are adapted to low levels of glucose and glutamine, two major PDAC-preferred nutrients, that however can become depleted in the tumor microenvironment at the core of tumors or under a short duration. I demonstrate that these adapted cells are able to synthesize glutamine by utilizing amino acids (branch-chain amino acid-Leucine, and glutamate), and the activity was correlated to the enhanced glutamine synthetase (GS) protein expression. While starving cells with glucose and glutamine abolished mTORC1 activity in parental cells, adapted cells are able to maintain their anabolic processes by maintaining the activation of mTORC1 signaling, which accounts for their proliferative advantage during nutrient starvation. Lastly, I discover a novel role of mTORC1 signaling, which can stabilize GS protein

expression during nutrient starvation. Genetic and pharmacological approaches to inhibit GS suppress cell proliferation under nutrient-poor conditions, highlighting the possibility to target metabolic dependencies of GS in PDAC as a potential therapy to inhibit tumor progression.

In Chapter 3, I present some additional findings to explain how do adapted cells maintain constitutive activation of mTORC1 signaling. I also discuss the other metabolic alterations that can contribute to the adapted response. In addition, potential caveats and important future work will also be discussed.

In sum, my research highlights the importance of targeting glutamine synthesis as a potential therapeutic target in PDAC.

1.5 Reference

1. L. Rahib *et al.*, Projecting cancer incidence and deaths to 2030: the unexpected burden of thyroid, liver, and pancreas cancers in the United States. *Cancer research* **74**, 2913-2921 (2014).

2. M. Hidalgo, Pancreatic cancer. *New England Journal of Medicine* **362**, 1605-1617 (2010).

3. A. Vincent, J. Herman, R. Schulick, R. H. Hruban, M. Goggins, Pancreatic cancer. *The lancet* **378**, 607-620 (2011).

4. P. P. Provenzano *et al.*, Enzymatic targeting of the stroma ablates physical barriers to treatment of pancreatic ductal adenocarcinoma. *Cancer cell* **21**, 418-429 (2012).

5. C. Feig *et al.* (AACR, 2012).

6. M. Erkan, C. Reiser-Erkan, C. Michalski, J. Kleeff, Tumor microenvironment and progression of pancreatic cancer. *Exp Oncol* **32**, 128-131 (2010).

7. S. Yachida, C. Iacobuzio-Donahue, Evolution and dynamics of pancreatic cancer progression. *Oncogene* **32**, 5253 (2013).

8. S. R. Hingorani *et al.*, Trp53R172H and KrasG12D cooperate to promote chromosomal instability and widely metastatic pancreatic ductal adenocarcinoma in mice. *Cancer cell* **7**, 469-483 (2005).

9. A. V. Biankin *et al.*, Pancreatic cancer genomes reveal aberrations in axon guidance pathway genes. *Nature* **491**, 399 (2012).

10. N. J. Roberts *et al.*, Whole genome sequencing defines the genetic heterogeneity of familial pancreatic cancer. *Cancer discovery* **6**, 166-175 (2016).

11. A. E. Karnoub, R. A. Weinberg, Ras oncogenes: split personalities. *Nature reviews Molecular cell biology* **9**, 517 (2008).

12. S. Gysin, M. Salt, A. Young, F. McCormick, Therapeutic strategies for targeting ras proteins. *Genes & cancer* **2**, 359-372 (2011).

13. J. J. Kamphorst *et al.*, Human pancreatic cancer tumors are nutrient poor and tumor cells actively scavenge extracellular protein. *Cancer research* **75**, 544-553 (2015).

14. C. A. Lyssiotis, A. C. Kimmelman, Metabolic interactions in the tumor microenvironment. *Trends in cell biology* **27**, 863-875 (2017).

15. R. Kalluri, The biology and function of fibroblasts in cancer. *Nature Reviews Cancer* **16**, 582 (2016).

16. F. Guillaumond *et al.*, Strengthened glycolysis under hypoxia supports tumor symbiosis and hexosamine biosynthesis in pancreatic adenocarcinoma. *Proc Natl Acad Sci U S A* **110**, 3919-3924 (2013).

17. C. M. Sousa *et al.*, Pancreatic stellate cells support tumour metabolism through autophagic alanine secretion. *Nature* **536**, 479 (2016).

18. N. J. Zyromski *et al.*, Obesity potentiates the growth and dissemination of pancreatic cancer. *Surgery* **146**, 258-263 (2009).

19. K. A. Meyer *et al.*, Adipocytes promote pancreatic cancer cell proliferation via glutamine transfer. *Biochemistry and biophysics reports* **7**, 144-149 (2016).

20. C. J. Halbrook *et al.*, Macrophage-Released Pyrimidines Inhibit Gemcitabine Therapy in Pancreatic Cancer. *Cell Metabolism*, (2019).

21. N. N. Pavlova, C. B. Thompson, The Emerging Hallmarks of Cancer Metabolism. *Cell Metab* **23**, 27-47 (2016).

22. D. Gaglio *et al.*, Oncogenic K-Ras decouples glucose and glutamine metabolism to support cancer cell growth. *Molecular systems biology* **7**, 523 (2011).

23. R. Iurlaro, C. L. León-Annicchiarico, C. Muñoz-Pinedo, in *Methods in enzymology*. (Elsevier, 2014), vol. 542, pp. 59-80.

24. A. Nagarajan, P. Malvi, N. Wajapeyee, Oncogene-directed alterations in cancer cell metabolism. *Trends in cancer* **2**, 365-377 (2016).

25. H. Ying *et al.*, Oncogenic Kras maintains pancreatic tumors through regulation of anabolic glucose metabolism. *Cell* **149**, 656-670 (2012).

26. J. Son *et al.*, Glutamine supports pancreatic cancer growth through a KRAS-regulated metabolic pathway. *Nature* **496**, 101 (2013).

27. D. E. Biancur, A. C. Kimmelman, The plasticity of pancreatic cancer metabolism in tumor progression and therapeutic resistance. *Biochimica et Biophysica Acta (BBA)-Reviews on Cancer*, (2018).

28. I. Dikic, Z. Elazar, Mechanism and medical implications of mammalian autophagy. *Nature Reviews Molecular Cell Biology*, 1 (2018).

29. I. G. Ganley *et al.*, ULK1· ATG13· FIP200 complex mediates mTOR signaling and is essential for autophagy. *Journal of Biological Chemistry* **284**, 12297-12305 (2009).

30. N. Hosokawa *et al.*, Nutrient-dependent mTORC1 association with the ULK1–Atg13–FIP200 complex required for autophagy. *Molecular biology of the cell* **20**, 1981-1991 (2009).

31. C. H. Jung *et al.*, ULK-Atg13-FIP200 complexes mediate mTOR signaling to the autophagy machinery. *Molecular biology of the cell* **20**, 1992-2003 (2009).

32. J. Kim, M. Kundu, B. Viollet, K.-L. Guan, AMPK and mTOR regulate autophagy through direct phosphorylation of Ulk1. *Nature cell biology* **13**, 132 (2011).

33. L. Shang *et al.*, Nutrient starvation elicits an acute autophagic response mediated by Ulk1 dephosphorylation and its subsequent dissociation from AMPK. *Proceedings of the National Academy of Sciences* **108**, 4788-4793 (2011).

34. S. Yang *et al.*, Pancreatic cancers require autophagy for tumor growth. *Genes & development*, (2011).

35. R. M. Perera *et al.*, Transcriptional control of autophagy–lysosome function drives pancreatic cancer metabolism. *Nature* **524**, 361 (2015).

36. M. T. Rosenfeldt *et al.*, p53 status determines the role of autophagy in pancreatic tumour development. *Nature* **504**, 296 (2013).

37. A. Yang *et al.*, Autophagy is critical for pancreatic tumor growth and progression in tumors with p53 alterations. *Cancer discovery*, (2014).

38. C. Commisso *et al.*, Macropinocytosis of protein is an amino acid supply route in Ras-transformed cells. *Nature* **497**, 633 (2013).

39. S. M. Davidson *et al.*, Direct evidence for cancer-cell-autonomous extracellular protein catabolism in pancreatic tumors. *Nature medicine* **23**, 235 (2017).

40. B. Faubert *et al.*, Lactate metabolism in human lung tumors. *Cell* **171**, 358-371. e359 (2017).

41. S. M. Davidson *et al.*, Environment impacts the metabolic dependencies of Ras-driven non-small cell lung cancer. *Cell metabolism* **23**, 517-528 (2016).

42. C. Nicholas, Hypoxia, HIF1 and glucose metabolism in the solid tumor. *Nat Rev Cancer* **8**, 705-713 (2008).

43. J.-w. Kim, I. Tchernyshyov, G. L. Semenza, C. V. Dang, HIF-1-mediated expression of pyruvate dehydrogenase kinase: a metabolic switch required for cellular adaptation to hypoxia. *Cell metabolism* **3**, 177-185 (2006).

44. E. Furuta *et al.*, Fatty acid synthase gene is up-regulated by hypoxia via activation of Akt and sterol regulatory element binding protein-1. *Cancer research* **68**, 1003-1011 (2008).

45. I. Mylonis *et al.*, Hypoxia causes triglyceride accumulation by HIF-1-mediated stimulation of lipin 1 expression. *J Cell Sci* **125**, 3485-3493 (2012).

46. J. R. Cantor *et al.*, Physiologic medium rewires cellular metabolism and reveals uric acid as an endogenous inhibitor of UMP synthase. *Cell* **169**, 258-272. e217 (2017).

47. J. V. Voorde *et al.*, Improving the metabolic fidelity of cancer models with a physiological cell culture medium. *Science advances* **5**, eaau7314 (2019).

48. M. A. Lancaster, J. A. Knoblich, Organogenesis in a dish: modeling development and disease using organoid technologies. *Science* **345**, 1247125 (2014).

49. D. Gao *et al.*, Organoid cultures derived from patients with advanced prostate cancer. *Cell* **159**, 176-187 (2014).

50. S. F. Boj *et al.*, Organoid models of human and mouse ductal pancreatic cancer. *Cell* **160**, 324-338 (2015).

51. H. Xu *et al.*, Organoid technology and applications in cancer research. *Journal of hematology & oncology* **11**, 116 (2018).

52. G. Vlachogiannis *et al.*, Patient-derived organoids model treatment response of metastatic gastrointestinal cancers. *Science* **359**, 920-926 (2018).

53. R. Kostadinova *et al.*, A long-term three dimensional liver co-culture system for improved prediction of clinically relevant drug-induced hepatotoxicity. *Toxicology and applied pharmacology* **268**, 1-16 (2013).

54. Q. Meng, Three-dimensional culture of hepatocytes for prediction of drug-induced hepatotoxicity. *Expert opinion on drug metabolism & toxicology* **6**, 733-746 (2010).

55. C. Pauli *et al.*, Personalized in vitro and in vivo cancer models to guide precision medicine. *Cancer discovery* **7**, 462-477 (2017).

56. O. Warburg, F. Wind, E. Negelein, The metabolism of tumors in the body. *The Journal of general physiology* **8**, 519 (1927).

57. O. H. Warburg, *The metabolism of tumours: investigations from the Kaiser Wilhelm Institute for Biology, Berlin-Dahlem*. (Constable & Company Limited, 1930).

58. S. W. House, O. Warburg, D. Burk, A. L. Schade, On respiratory impairment in cancer cells. *Science* **124**, 267-272 (1956).

59. W. H. Koppenol, P. L. Bounds, C. V. Dang, Otto Warburg's contributions to current concepts of cancer metabolism. *Nature Reviews Cancer* **11**, 325 (2011).

60. P. P. Hsu, D. M. Sabatini, Cancer cell metabolism: Warburg and beyond. *Cell* **134**, 703-707 (2008).

61. L. Kostakoglu, H. Agress Jr, S. J. Goldsmith, Clinical role of FDG PET in evaluation of cancer patients. *Radiographics* **23**, 315-340 (2003).

62. N. Hay, Reprogramming glucose metabolism in cancer: can it be exploited for cancer therapy? *Nature Reviews Cancer* **16**, 635 (2016).

63. K. C. Patra, N. Hay, The pentose phosphate pathway and cancer. *Trends in biochemical sciences* **39**, 347-354 (2014).

64. F. Chiaradonna, F. Ricciardiello, R. Palorini, The nutrient-sensing hexosamine biosynthetic pathway as the hub of cancer metabolic rewiring. *Cells* **7**, 53 (2018).

65. J. W. Locasale, Serine, glycine and one-carbon units: cancer metabolism in full circle. *Nature reviews Cancer* **13**, 572 (2013).

66. G. Bergers, L. E. Benjamin, Angiogenesis: tumorigenesis and the angiogenic switch. *Nature reviews cancer* **3**, 401 (2003).

67. D. Fukumura, R. K. Jain, Tumor microvasculature and microenvironment: targets for anti-angiogenesis and normalization. *Microvascular research* **74**, 72-84 (2007).

68. A. Hirayama *et al.*, Quantitative metabolome profiling of colon and stomach cancer microenvironment by capillary electrophoresis time-of-flight mass spectrometry. *Cancer research* **69**, 4918-4925 (2009).

69. K. Birsoy *et al.*, Metabolic determinants of cancer cell sensitivity to glucose limitation and biguanides. *Nature* **508**, 108 (2014).

70. C. Huang *et al.*, Lactate promotes resistance to glucose starvation via upregulation of Bcl-2 mediated by mTOR activation. *Oncology reports* **33**, 875-884 (2015).

71. E. R. Still, M. O. Yuneva, Hopefully devoted to Q: targeting glutamine addiction in cancer. *British journal of cancer* **116**, 1375 (2017).

72. P. G. Petronini, S. Urbani, R. Alfieri, A. F. Borghetti, G. G. Guidotti, Cell susceptibility to apoptosis by glutamine deprivation and rescue: Survival and apoptotic death in cultured lymphoma-leukemia cell lines. *Journal of cellular physiology* **169**, 175-185 (1996).

73. M. Yuneva, N. Zamboni, P. Oefner, R. Sachidanandam, Y. Lazebnik, Deficiency in glutamine but not glucose induces MYC-dependent apoptosis in human cells. *The Journal of cell biology* **178**, 93-105 (2007).

74. L. A. Timmerman *et al.*, Glutamine sensitivity analysis identifies the xCT antiporter as a common triple-negative breast tumor therapeutic target. *Cancer cell* **24**, 450-465 (2013).

75. D. Yu *et al.*, Kidney-type glutaminase (GLS1) is a biomarker for pathologic diagnosis and prognosis of hepatocellular carcinoma. *Oncotarget* **6**, 7619 (2015).

76. P. Gao *et al.*, c-Myc suppression of miR-23a/b enhances mitochondrial glutaminase expression and glutamine metabolism. *Nature* **458**, 762 (2009).

77. W. Hu *et al.*, Glutaminase 2, a novel p53 target gene regulating energy metabolism and antioxidant function. *Proceedings of the National Academy of Sciences* **107**, 7455-7460 (2010).

78. A. Cadoret *et al.*, New targets of β-catenin signaling in the liver are involved in the glutamine metabolism. *Oncogene* **21**, 8293 (2002).

79. A. Schousboe, S. Scafidi, L. K. Bak, H. S. Waagepetersen, M. C. McKenna, in *Glutamate and ATP at the Interface of Metabolism and Signaling in the Brain*. (Springer, 2014), pp. 13-30.

80. S. Tardito *et al.*, Glutamine synthetase activity fuels nucleotide biosynthesis and supports growth of glutamine-restricted glioblastoma. *Nature cell biology* **17**, 1556 (2015).

81. A. J. Bott *et al.*, Oncogenic Myc induces expression of glutamine synthetase through promoter demethylation. *Cell metabolism* **22**, 1068-1077 (2015).

82. A. O. A. Michael *et al.*, Inhibiting Glutamine-Dependent mTORC1 Activation Ameliorates Liver Cancers Driven by β-Catenin Mutations. *Cell Metabolism*, (2019).

83. S. Loeppen *et al.*, Overexpression of glutamine synthetase is associated with β-catenin-mutations in mouse liver tumors during promotion of hepatocarcinogenesis by phenobarbital. *Cancer research* **62**, 5685-5688 (2002).

84. H.-N. Kung, J. R. Marks, J.-T. Chi, Glutamine synthetase is a genetic determinant of cell type–specific glutamine independence in breast epithelia. *PLoS genetics* **7**, e1002229 (2011).

85. L. Yang *et al.*, Targeting stromal glutamine synthetase in tumors disrupts tumor microenvironment-regulated cancer cell growth. *Cell metabolism* **24**, 685-700 (2016).

86. T. Hakvoort *et al.*, Pivotal role of glutamine synthetase in ammonia detoxification. *Hepatology* **65**, 281-293 (2017).

87. B. H. Sohn, I. Y. Park, J.-H. Shin, S. Y. Yim, J.-S. Lee, Glutamine synthetase mediates sorafenib sensitivity in β-catenin-active hepatocellular carcinoma cells. *Experimental & molecular medicine* **50**, e421 (2018).

88. K. E. Van Der Vos *et al.*, Modulation of glutamine metabolism by the PI (3) K–PKB–FOXO network regulates autophagy. *Nature cell biology* **14**, 829 (2012).

89. T. V. Nguyen *et al.*, Glutamine Triggers Acetylation-Dependent Degradation of Glutamine Synthetase via the Thalidomide Receptor Cereblon. *Mol Cell* **61**, 809-820 (2016).

90. M. Hassanein *et al.*, Targeting SLC1a5-mediated glutamine dependence in non-small cell lung cancer. *International journal of cancer* **137**, 1587-1597 (2015).

91. M. Lampa *et al.*, Glutaminase is essential for the growth of triple-negative breast cancer cells with a deregulated glutamine metabolism pathway and its suppression synergizes with mTOR inhibition. *PloS one* **12**, e0185092 (2017).

92. Z. Song, B. Wei, C. Lu, P. Li, L. Chen, Glutaminase sustains cell survival via the regulation of glycolysis and glutaminolysis in colorectal cancer. *Oncology letters* **14**, 3117-3123 (2017).

93. D. E. Biancur *et al.*, Compensatory metabolic networks in pancreatic cancers upon perturbation of glutamine metabolism. *Nature communications* **8**, 15965 (2017).

94. H. Baker, A. Sidorowicz, S. Sehgal, C. VÉZINA, Rapamycin (AY-22, 989), a new antifungal antibiotic. *The Journal of antibiotics* **31**, 539-545 (1978).

95. J. Kim, K.-L. Guan, mTOR as a central hub of nutrient signalling and cell growth. *Nature cell biology* **21**, 63 (2019).

96. A. J. Valvezan, B. D. Manning, Molecular logic of mTORC1 signalling as a metabolic rheostat. *Nature Metabolism*, 1 (2019).

97. B. C. Grabiner *et al.*, A diverse array of cancer-associated MTOR mutations are hyperactivating and can predict rapamycin sensitivity. *Cancer discovery* **4**, 554-563 (2014).

98. Y. Zhang *et al.*, A pan-cancer proteogenomic atlas of PI3K/AKT/mTOR pathway alterations. *Cancer cell* **31**, 820-832. e823 (2017).

99. D. M. Sabatini, Twenty-five years of mTOR: Uncovering the link from nutrients to growth. *Proceedings of the National Academy of Sciences* **114**, 11818-11825 (2017).

100. D.-H. Kim *et al.*, mTOR interacts with raptor to form a nutrient-sensitive complex that signals to the cell growth machinery. *Cell* **110**, 163-175 (2002).

101. E. Kim, P. Goraksha-Hicks, L. Li, T. P. Neufeld, K.-L. Guan, Regulation of TORC1 by Rag GTPases in nutrient response. *Nature cell biology* **10**, 935 (2008).

102. N. Siddiqui, N. Sonenberg, Signalling to eIF4E in cancer. *Biochemical Society transactions* **43**, 763-772 (2015).

103. X. M. Ma, J. Blenis, Molecular mechanisms of mTOR-mediated translational control. *Nature reviews Molecular cell biology* **10**, 307 (2009).

104. A. N. Lane, T. W.-M. Fan, Regulation of mammalian nucleotide metabolism and biosynthesis. *Nucleic acids research* **43**, 2466-2485 (2015).

105. M. Evert *et al.*, V-AKT murine thymoma viral oncogene homolog/mammalian target of rapamycin activation induces a module of metabolic changes contributing to growth in insulin-induced hepatocarcinogenesis. *Hepatology* **55**, 1473-1484 (2012).

106. A. Juvekar *et al.*, Phosphoinositide 3-kinase inhibitors induce DNA damage through nucleoside depletion. *Proceedings of the National Academy of Sciences* **113**, E4338-E4347 (2016).

107. I. Ben-Sahra, G. Hoxhaj, S. J. Ricoult, J. M. Asara, B. D. Manning, mTORC1 induces purine synthesis through control of the mitochondrial tetrahydrofolate cycle. *Science* **351**, 728-733 (2016).

108. A. M. Robitaille *et al.*, Quantitative phosphoproteomics reveal mTORC1 activates de novo pyrimidine synthesis. *Science* **339**, 1320-1323 (2013).

109. I. Ben-Sahra, J. J. Howell, J. M. Asara, B. D. Manning, Stimulation of de novo pyrimidine synthesis by growth signaling through mTOR and S6K1. *Science*, 1228792 (2013).

110. J. L. Owen *et al.*, Insulin stimulation of SREBP-1c processing in transgenic rat hepatocytes requires p70 S6-kinase. *Proceedings of the National Academy of Sciences* **109**, 16184-16189 (2012).

111. J. L. Yecies *et al.*, Akt stimulates hepatic SREBP1c and lipogenesis through parallel mTORC1-dependent and independent pathways. *Cell metabolism* **14**, 21-32 (2011).

112. S. J. Ricoult, J. L. Yecies, I. Ben-Sahra, B. D. Manning, Oncogenic PI3K and K-Ras stimulate de novo lipid synthesis through mTORC1 and SREBP. *Oncogene* **35**, 1250 (2016).

113. J. A. Martina, Y. Chen, M. Gucek, R. Puertollano, MTORC1 functions as a transcriptional regulator of autophagy by preventing nuclear transport of TFEB. *Autophagy* **8**, 903-914 (2012).

114. A. Roczniak-Ferguson *et al.*, The transcription factor TFEB links mTORC1 signaling to transcriptional control of lysosome homeostasis. *Sci. Signal.* **5**, ra42-ra42 (2012).

115. W. Palm *et al.*, The utilization of extracellular proteins as nutrients is suppressed by mTORC1. *Cell* **162**, 259-270 (2015).

116. Y. Zhang *et al.*, Coordinated regulation of protein synthesis and degradation by mTORC1. *Nature* **513**, 440 (2014).

117. J. Zhao, B. Zhai, S. P. Gygi, A. L. Goldberg, mTOR inhibition activates overall protein degradation by the ubiquitin proteasome system as well as by autophagy. *Proceedings of the National Academy of Sciences* **112**, 15790-15797 (2015).

118. A. Rousseau, A. Bertolotti, An evolutionarily conserved pathway controls proteasome homeostasis. *Nature* **536**, 184 (2016).

119. D. R. Alessi *et al.*, Characterization of a 3-phosphoinositide-dependent protein kinase which phosphorylates and activates protein kinase Bα. *Current biology* **7**, 261-269 (1997).

120. K. Inoki, Y. Li, T. Zhu, J. Wu, K.-L. Guan, TSC2 is phosphorylated and inhibited by Akt and suppresses mTOR signalling. *Nature cell biology* **4**, 648 (2002).

121. B. D. Manning, A. R. Tee, M. N. Logsdon, J. Blenis, L. C. Cantley, Identification of the tuberous sclerosis complex-2 tumor suppressor gene product tuberin as a target of the phosphoinositide 3-kinase/akt pathway. *Molecular cell* **10**, 151-162 (2002).

122. X. Long, Y. Lin, S. Ortiz-Vega, K. Yonezawa, J. Avruch, Rheb binds and regulates the mTOR kinase. *Current biology* **15**, 702-713 (2005).

123. H. Yang *et al.*, Mechanisms of mTORC1 activation by RHEB and inhibition by PRAS40. *Nature* **552**, 368 (2017).

124. Y. Sancak *et al.*, Ragulator-Rag complex targets mTORC1 to the lysosomal surface and is necessary for its activation by amino acids. *Cell* **141**, 290-303 (2010).

125. M. Rebsamen *et al.*, SLC38A9 is a component of the lysosomal amino acid sensing machinery that controls mTORC1. *Nature* **519**, 477 (2015).

126. G. A. Wyant *et al.*, mTORC1 activator SLC38A9 is required to efflux essential amino acids from lysosomes and use protein as a nutrient. *Cell* **171**, 642-654. e612 (2017).

127. J. Jung, H. M. Genau, C. Behrends, Amino acid-dependent mTORC1 regulation by the lysosomal membrane protein SLC38A9. *Molecular and cellular biology* **35**, 2479-2494 (2015).

128. S. Wang *et al.*, Lysosomal amino acid transporter SLC38A9 signals arginine sufficiency to mTORC1. *Science* **347**, 188-194 (2015).

129. A. Parmigiani *et al.*, Sestrins inhibit mTORC1 kinase activation through the GATOR complex. *Cell reports* **9**, 1281-1291 (2014).

130. R. L. Wolfson *et al.*, Sestrin2 is a leucine sensor for the mTORC1 pathway. *Science* **351**, 43-48 (2016).

131. L. Chantranupong *et al.*, The CASTOR proteins are arginine sensors for the mTORC1 pathway. *Cell* **165**, 153-164 (2016).

132. X. Gu *et al.*, SAMTOR is an S-adenosylmethionine sensor for the mTORC1 pathway. *Science* **358**, 813-818 (2017).

Chapter 2:

Glutamine synthesis is a metabolic dependency in pancreatic cancer cells adapted in a nutrient-deprived environment

This chapter is adapted from:

Pei-Yun Tsai, Min-Sik Lee, Peter DelNero, Ashley Adler, Caroline Lewis, Daniel S. Hitchcock, Meeta Mistry.

Manuscript in preparation.

2.1 Abstract

Pancreatic ductal adenocarcinoma (PDAC) accounts for 90% of pancreatic cancer, and has a survival rate of only 8%. One of the difficulties for targeting this cancer is its unique tumor microenvironment that is characterized by desmoplasia and hypovascularization, resulting in limited nutrient availability and drug efficacy. Although some cancer cells might experience a shortage of nutrients, the capacity of PDAC cells to adapt to limited -glucose (Glc) and -glutamine (Gln) conditions is poorly understood. Here, we derived PDAC cells that adapted to low Glc-low Gln (L-L) conditions. We demonstrated that these cells induce glutamine synthesis to overcome this nutrient-starved environment. We further showed that the adapted cells maintain activation of the mechanistic target of rapamycin complex 1 (mTORC1), which can prevent proteasomal degradation of glutamine synthetase (GS). Genetic and pharmacological approaches to inhibit GS suppressed cell proliferation under nutrient-poor, but not nutrient-replete conditions. Our findings highlight GS as a metabolic dependency and identify it as a potential therapeutic target in PDAC.

2.2 Introduction

It has been shown that PDAC exhibits lower levels of glucose (Glc) and glutamine (Gln), in comparison to the surrounding benign tissue (*1*), and that these two nutrients are essential for PDAC cells *in vitro* (*2*). To overcome and thrive under nutrient-deprived conditions, PDAC rewires its metabolism. This includes increased glycolysis (*3, 4*), altered glutamine metabolism (*2*), enhanced basal autophagy (*5-7*), and increased macropinocytic activity (*8*). Emerging studies have demonstrated that cancer cells exhibit metabolic plasticity under different nutrient-limiting

conditions (*9-12*). However, it remains unclear how PDAC cells rewire their metabolism and adapt to glucose- and glutamine-starved conditions when cells undergo nutrient shortage *in vivo* (*13*).

To derive PDAC cells that can adapt to adverse conditions, we exposed 7 PDAC cell lines (AsPC-1, MIAPaCa-2, BxPC-3, PANC-1, HPAC, SUIT-2, and PA-TU-8988T, here referred to as 8988T) to a medium containing low Glc (0.5 mM) and low Gln (0.1 mM), with 10% dialyzed fetal bovine serum (FBS). Despite replenishing the L-L medium every 2-3 days, most PDAC cells died in these harsh conditions. However, a small number of SUIT-2 and 8988T cells were able to survive, and even proliferate following 2 weeks of selection. We then derived several single clones from this heterogenous population that we described as "adapted clones" (or A-C) (Fig. 2.1) given their resistance to L-L conditions, and we passaged them every 3-4 days for the rest of the experiments. On the other hand, single clones derived from the counterpart conditions, which are high Glc (11 mM) and high Gln (2 mM) plus 10% dialyzed FBS, or "H-H conditions," are described as "non-adapted clones" (or NA-C) (Fig. 2.1).

2.3 Material and Methods

Reagents

Antibodies for western blotting: pThr389-S6K (Cell Signaling technologies CST-4691; 1:1000), S6K (SC-8418; 1:1000), LC3 (CST-2775; 1:1000), GAPDH (SC-25778; 1:5000), β-Actin (Santa Cruz, SC-47778, 1:20000), pS65-4EBP1 (CST-9451; 1:1000), 4EBP1 (CST-9644; 1:1000), pS1859-CAD (CST-12662; 1:1000), CAD (CST-11933; 1:1000), pT308-AKT (CST-4056; 1:1000), pS473-AKT (CST-4058; 1:1000), GS (BD Bioscience, BD-61057; 1:1000), BCAT1 (Abcam, ab-107191; 1:1000), BCAT2 (CST-9432; 1:1000), GOT1 (Novus Biologicals, NBP1-54778; 1:1000), GOT2 (ab171739; 1:1000), GLUD1 (Proteintech, 14299-1-AP; 1:1000).

Cell culture

Human PDA cell line-SUIT-2 were from Japanese Collection of Research Bioresources, and PA-TU-8988T were from German Collection of Microorganisms and Cell culture. Both cell lines were authenticated by STR profiling at ATCC. All cells were maintained at 37°C in a humidified incubator with 5% CO2 and were grown in RPMI medium lacking glucose and glutamine (US Biological-R9011) that is supplemented with glucose (Thermo Fisher Scientific-A2494001) and glutamine (Life Technologies-25030-81), at the indicated concentrations. Media were supplemented with 10% dialyzed fetal bovine serum (Sigma-Aldrich F0392) in all the experiments. Non-adapted clones were maintained in 11 mM of glucose and 2 mM glutamine, whereas adapted clones were maintained in 0.5 mM of glucose and 0.1 mM of glutamine.

Cell proliferation and cell death assay

Three thousand cells were plated per well in 96-well plates a day before subjecting them to treatment conditions. Cells were then washed with PBS and treated with the experimental conditions along with 2 μg/ml Propidium Iodide for 7 days without refreshing the media. Live or dead cells were counted by Celigo Image Cytometer (Nexcelom Bioscience). Cells numbers were normalized to day 1 and presented as relative cell numbers.

Clonogenic assay

600 cells were plated per well in 6-well plates before subjecting them to treatment conditions for 7-10 days, depending on the experiment. Colony numbers were quantified by Celigo Image Cytometer (Nexcelom Bioscience).

Sphere formation assay

50 cells were plated per well in 96-well plates and supplemented with 4% matrigel, 16-24 hours before subjecting them to treatment conditions. Cells were then washed gently with PBS before being treated according to the experimental conditions. Spheres were counted after 7-10 days by Celigo Image Cytometer (Nexelom Bioscience).

Radio-isotope experiment

U-^{14}C-aspartic acid was purchased from PerkinElmer, and 1 Ci was added to each well in H-H or L-L conditions for 40 hours. After washing the cells with PBS, DNA was collected by PureLink Genomic DNA mini kit (Invitrogen). DNA samples were mixed with scintillation buffer, and

radioactivity was counted by scintillation counter. The numbers from Disintegrations per minute (DPM) were used to calculate between samples after normalized to the DNA quantity first, and then compared to the count numbers in parental NA cells under L-L conditions. The values presented as a fold change.

Metabolite tracing and extraction

For the ^{15}N-ammonium chloride stable-isotope experiment, cells were plated in quadruplicates and treated for 24 hours with RPMI lacking glucose and glutamine (US Biological) that was supplemented with glucose and glutamine at H-H or L-L concentrations. The cells were concomitantly labeled with ^{15}N-ammonium chloride (0.8 mM). For ^{15}N-glutamic acid (0.1 mM) or ^{15}N-Leucine (0.4 mM) experiments, cells were treated for 24 hours with RPMI lacking glucose, glutamine, and amino acids (US Biological) and supplemented with glucose and glutamine at H-H or L-L conditions. Media were supplemented with individual amino acids up to the concentration present in standard RPMI. All the stable isotopes were purchased from Cambridge Isotope Laboratories. After treating the cells for the indicated timepoints, metabolites were extracted according to the following protocol. Cells were washed with cold PBS and metabolites were extracted with extraction solution (80% methanol containing a mixture of internal amino acid standards at 90.0 nM each) on dry ice, then vortexed for 10 min at 4C and centrifuged at top speed (10 min, 10,000 x g, 4C). Supernatants were then transferred to chilled Eppendorf tubes and dried with a SpeedVac. Dried extracts were suspended in 100 µl of water and centrifuged at top speed at 10 min, and the supernatants were analyzed with Liquid Chromatography/Mass Spectrometry (LC/MS).

Mouse work for orthotopic transplants

All animal studies and procedures were approved by the Animal Care and Use Committee at Boston Children's Hospital. For orthotopic xenografts, 750,000 cells suspended in 25 μl of 33% Matrigel (BD Biosciences 356231) in HBSS were injected into the pancreata of B6.129S7-Rag1tm1Mom/ J mice termed Rag -/- mice (Jackson Laboratory #002216). Mice were euthanized 33 days following the injections and tumors were harvested and measured using a digital caliper. Tumor volumes were estimated according to the ellipsoid formula: 4/3 x π x (a/2 x b/2 x c/2).

Statistical Analysis

Date are presented as mean ± SD or ± SEM, unless otherwise indicated. When comparing two groups, a two-tailed non-paired Student *t* test was conducted. For three or more groups, one-way ANOVA was conducted except for proliferation curves, where two-way ANOVA was conducted. ANOVA was followed by post hoc Tukey's multiple-comparison test. $P < 0.05$ was considered statistically significant.

2.4 Results

2.4.1 Adapted clones (A-C) display a proliferative advantage over non-adapted clones (NA-C) under L-L conditions.

All clones, adapted and non-adapted, proliferated at comparable rates under H-H conditions (Fig. 2.2a) and exhibited a low percentage of cell death (Fig. 2.2b). However, non-adapted clones displayed growth inhibition (Fig. 2.3a) and increased cell death (Fig. 2.3b) under L-L conditions. In contrast, adapted clones had an increased rate of proliferation under these harsh conditions (Fig. 2.3a, b). Moreover, adapted clones formed more colonies than adapted clones under L-L conditions (Fig. 2.3c), but no differences were observed under H-H conditions (Fig. 2.2c). In a three-dimensional (3D) assay where media were supplemented with 4% matrigel, only 8988T adapted clones, but not their non-adapted controls were able to form spheres under both L-L (Fig. 2.3d) and H-H conditions (Fig. 2.2d) (Fig. 2.2d, 2.3d). Interestingly, although SUIT-2 adapted clones and non-adapted clones formed the same numbers of spheres, adapted SUIT-2 clones tended to form larger spheres than non-adapted clones in L-L conditions. This differential phenotype between SUIT-2 and 8988T clonal cells suggests that nutrient deprivation can cause metabolic adaptations that enhance cellular fitness, albeit this fitness might be expressed differently in these cell lines.

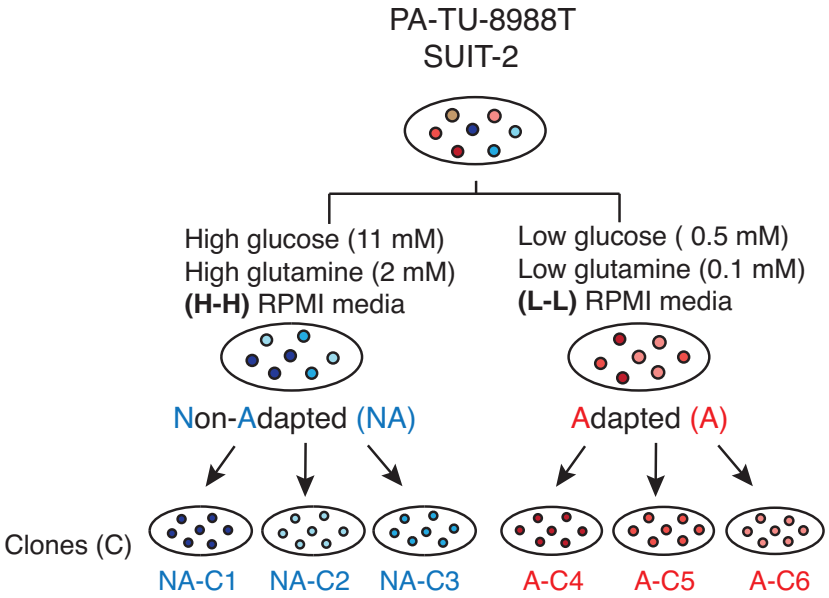

Figure 2.1. Schematic diagram of PDAC clones derived under chronic low glucose-low glutamine (L-L) conditions.

PDAC cell lines (8988T, SUIT-2) were subjected to low glucose (0.5 mM)-low glutamine (0.1 mM) or "L-L" media, and then sub-cultured every 3-4 days under these conditions are described as "adapted" cells. Three homogenous clonal cells were selected from the heterogenous adapted cells, and are described as "Adapted Clones (A-C)": A-C4, -C5, -C6. Counterparts of the adapted cells are cells derived from the same parental cells, that were however cultured in high glucose (11 mM)-high glutamine (2 mM) or "H-H" media. Three clonal cells that were derived from H-H media are described as "Non-Adapted clones" (NA-C): NA-C1, -C2, -C3. Red represents cells adapted from L-L conditions; Blue represents cells adapted from H-H conditions.

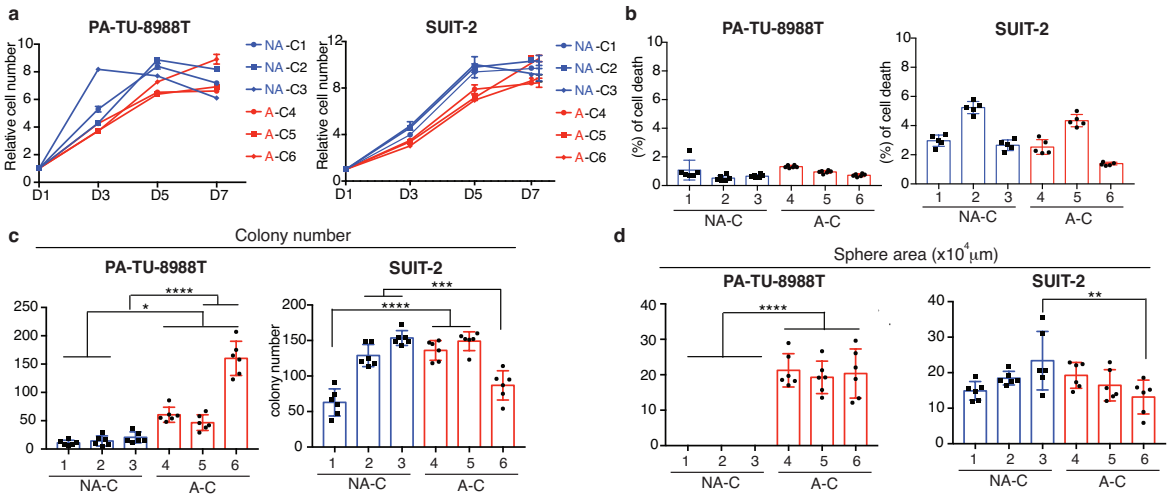

Figure 2.2. Non-adapted clones (NA-C) and adapted clones (A-C) displays similar proliferative phenotype under H-H conditions.

a, Proliferation curves of NA-C (NA-C1, -C2, -C3) and A-C (A-C4, -C5, -C6) from 8988T or SUIT-2 that were subjected to H-H conditions for 7 days (n=6). Cell numbers were measured by the Celigo machine (Nexcelom Bioscience), and the numbers are presented as a fold change that is relative to day 1. **b**, NA-C and A-C in 8988T and SUIT-2 were stained with the fluorescent Propidium Iodide (PI) dye as a marker for dead cells under H-H conditions. The percentage of cell death was measured by the Celigo machine after 4 days in H-H conditions (n=6). **c**, Colony numbers were measured upon H-H conditions for 10 days in 8988T clones or for 7 days in SUIT-2 clones by the Celigo machine (n=6). **d**, 3-dimention (3D) sphere areas were measured under H-H conditions plus 4% matrigel for 10 days in 8988T clones or 7 days in SUIT-2 clones (n=6). In **c** and **d**, data are shown as mean ± SD; *$P < 0.05$; **$P < 0.01$; ***$P < 0.001$; ****$P < 0.0001$.

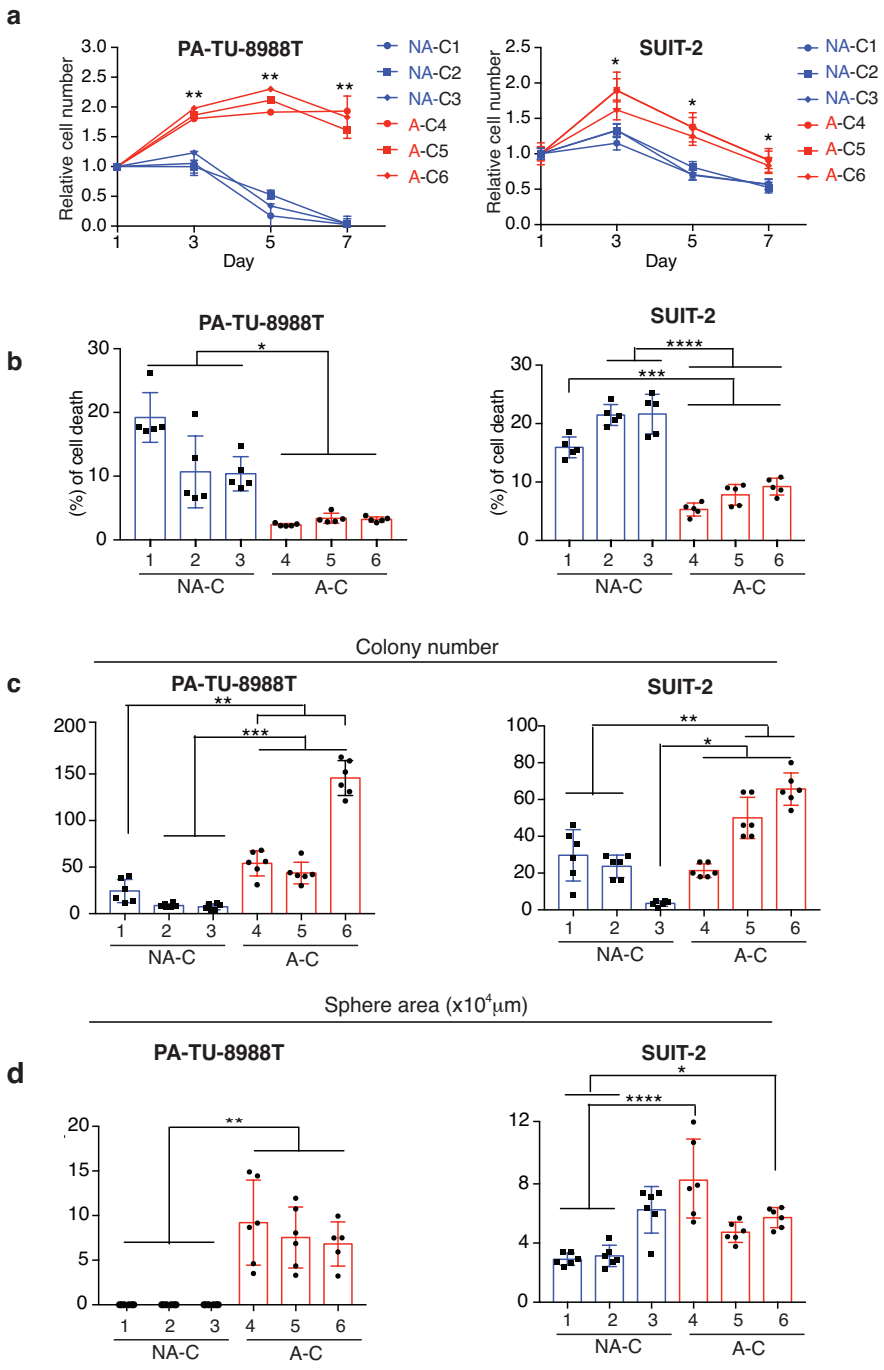

Figure 2.3. Adapted clones (A-C) exhibit a proliferative advantage over non-adapted clones (NA-C) under L-L conditions.

a, Proliferation curves of NA-C (NA-C1, -C2, -C3) and A-C (A-C4, -C4, -C5) from 8988T

Figure 2.3 (Continued)

and SUIT-2 that were subjected to L-L conditions for 7 days (n=6). Cell numbers were measured by Celigo machine (Nexcelom Bioscience), and the numbers are presented as fold change relative to day 1. **b**, NA-C and A-C in 8988T and SUIT-2 clones were stained with Propidium Iodide (PI) dye as a marker for the dead cells under L-L conditions. The percentage of cell death was measured by Celigo machine after 4 days in L-L conditions (n=6). **c**, Colony numbers were measured upon L-L conditions for 10 days in -8988T clones or for 7 days in SUIT-2 clones by Celigo machine (n=6). **d**, 3-dimension (3D) sphere areas were measured in 8988T clones upon H-H conditions plus 4% matrigel for 10 days or 7 days in SUIT-2 clones (n=6). In **c** and **d**, data are shown as mean ± SD; $*P < 0.05$; $**P < 0.01$; $***P < 0.001$; $****P < 0.0001$.

2.4.2 Adapted clones display elevated *de novo* pyrimidine synthesis along with mTORC1 activation under L-L conditions.

Autophagy and macropinocytosis are the two important nutrient acquisition pathways that have been shown to be elevated in pancreatic cancer cells (*5*-*8*). We performed experiments to access whether the proliferative phenotype in adapted clones under L-L conditions was due to increased autophagic and macropinocytotic activities. In our findings, adapted clones had either a similar or reduced autophagic flux compared to non-adapted clones (Fig. 2.4a b) under L-L conditions. In addition, adapted clones had reduced macropinocytotic activity compared to non-adapted clones (Fig. 2.4c).

To examine metabolic alterations between non-adapted clones and adapted clones, we performed a steady-state global metabolic profiling experiment. Although several metabolite levels (amino acids, glycolytic metabolites, and fatty acids) were altered under L-L conditions compared to H-H conditions independent of clones (Fig. 2.5), adapted clones displayed lower levels of amino acids and some nucleotide species in comparison to non-adapted clones under L-L conditions. On the other hand, metabolites in the TCA cycle were elevated in adapted clones. As expected, pathway enrichment analysis showed that purine and pyrimidine metabolism were significantly altered between adapted clones and non-adapted clones under L-L conditions (Fig. 2.6a). Within this pathway, nucleoside mono- or di-phosphates were lower in adapted clones compared to non-adapted clones (Fig. 2.6b). In contrast, PRPP, carbamoyl-aspartate, and tri-phosphates were increased in adapted clones. We reasoned that adapted clones might have enhanced nucleotide synthesis as well as enhanced nucleotide utilization to meet demands for proliferation as we have shown (Fig 2.3).

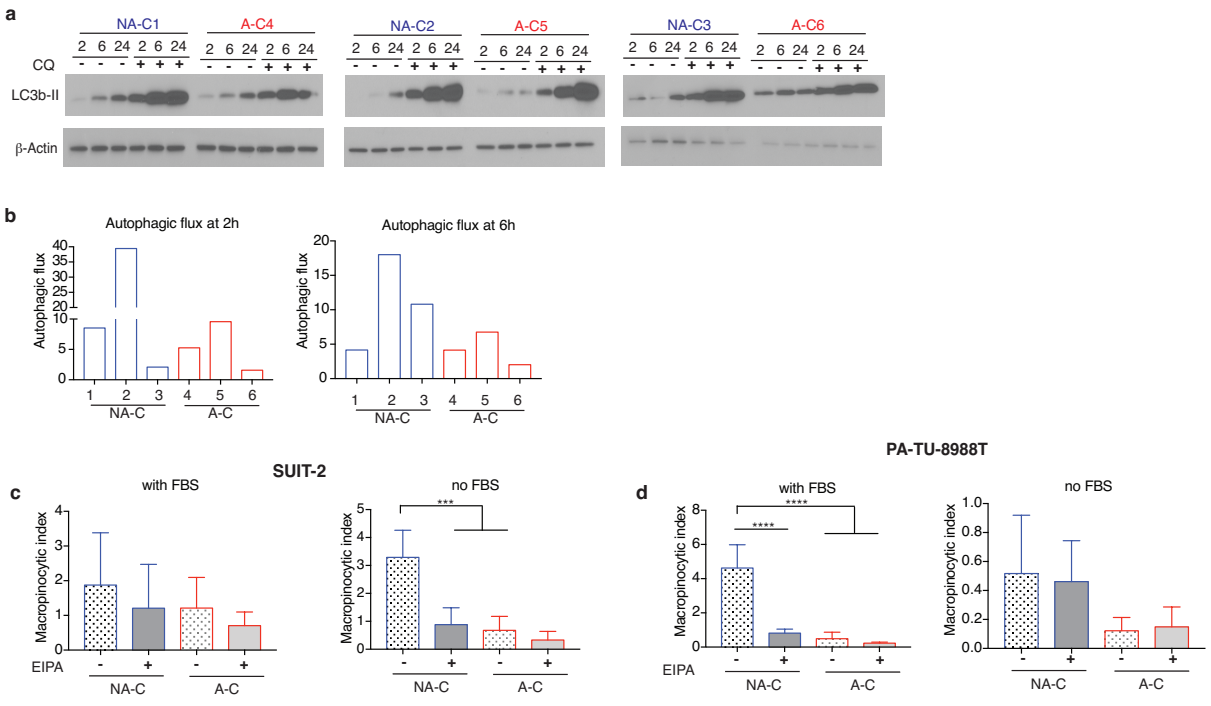

Figure 2.4. Adapted clones do not display increased autophagic flux and macropinocytosis activity.

a, Immunoblots of lipidated form of LC3, LC3-II in NA-C and A-C (SUIT-2) under L-L conditions with either DMSO control or lysosome inhibitor, chloroquine (CQ) (10 μM) treatment at the indicated timepoints. **b**, Quantification of the LC3-II levels from (**a)** with CQ treatment at the indicated timepoints (2 hours or 6 hours) compared to the same clones treated with DMSO control. The quantification is analyzed by ImageJ. **c**, Macropinocytic index (puncta number/cell number) are presented in NA-C1 and A-C4 in SUIT-2 (**a)** or 8988T (**b)** under L-L conditions either with or without 10% dialyzed FBS (n=5). EIPA (25 μM) is a known macropinocytosis inhibitor, used here as a positive control.

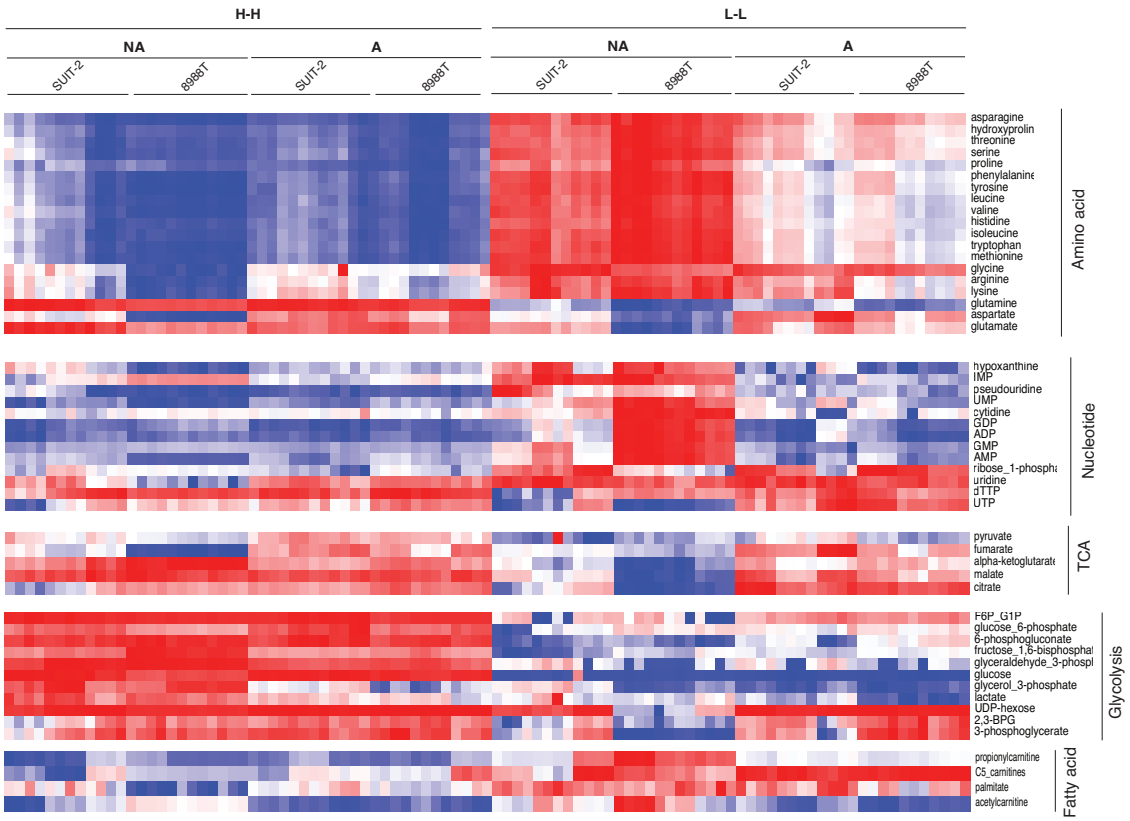

Fig. 2.5. Heatmap representing differential metabolite levels between non-adapted and adapted-clones treated with L-L media conditions.

Heatmap listing metabolites that reached statistical significance ($P < 0.05$ by t-test) among 4 groups (combined 8988T and SUIT-2): 3 clones each per cell line, either adapted or non-adapted, that were treated for 24 hours with either H-H or L-L conditions. Data were processed by Metaboanalyst 4.0 with the statistical analysis module. Red indicates increased levels, and blue indicates reduced levels within each group. (n=4 biological replicates per clone, except for A-C in 8988T cells, where n = 3).

To test this explanation, we performed a ^{14}C-aspartate labeling experiment given that the carbon on aspartate can contribute to the pyrimidine ring. We demonstrated that, adapted clones had elevation of *de novo* pyrimidine synthesis activities in comparison to non-adapted clones under L-L conditions (Fig 2.6c). As expected, the activities were lower than when clones were under H-H conditions.

It is well known that the mechanistic target of rapamycin complex 1 (mTORC1) is important for several anabolic processes, including protein, fatty acid, and nucleotide synthesis (*14-17*). Whereas all clones displayed activation of mTORC1 signaling upon H-H treatment for 24 hours, only adapted clones maintained mTORC1 activity under L-L conditions with increased phosphorylation of its downstream targets, ribosomal S6-Kinase (S6K) and eukaryotic translation initiation factor 4E-binding protein 1 (4E-BP1) (Fig. 2.6d). Adapted clones also showed increased S6K-mediated phosphorylation at Ser1859 of the multi-complex enzyme, carbamoyl-phosphate synthetase 2, aspartate transcarbamylase, and dihydroorotate (CAD), which is responsible for *de novo* pyrimidine synthesis (*18*). On the other hand, although mTORC2 signaling was elevated in non-adapted clones with increased phosphorylation in downstream target, p-AKT at Ser473, the mTORC1 signaling was completely abolished under L-L conditions (Fig. 2.7). To reason whether the activation of mTORC1 activity in adapted clones was due to pre-existing genetic mutations in adapted clones, or the result of metabolic adaptation, perhaps due to epigenetic alterations, we assayed for the reversal of adaptation by sub-culturing adapted clones in H-H conditions for

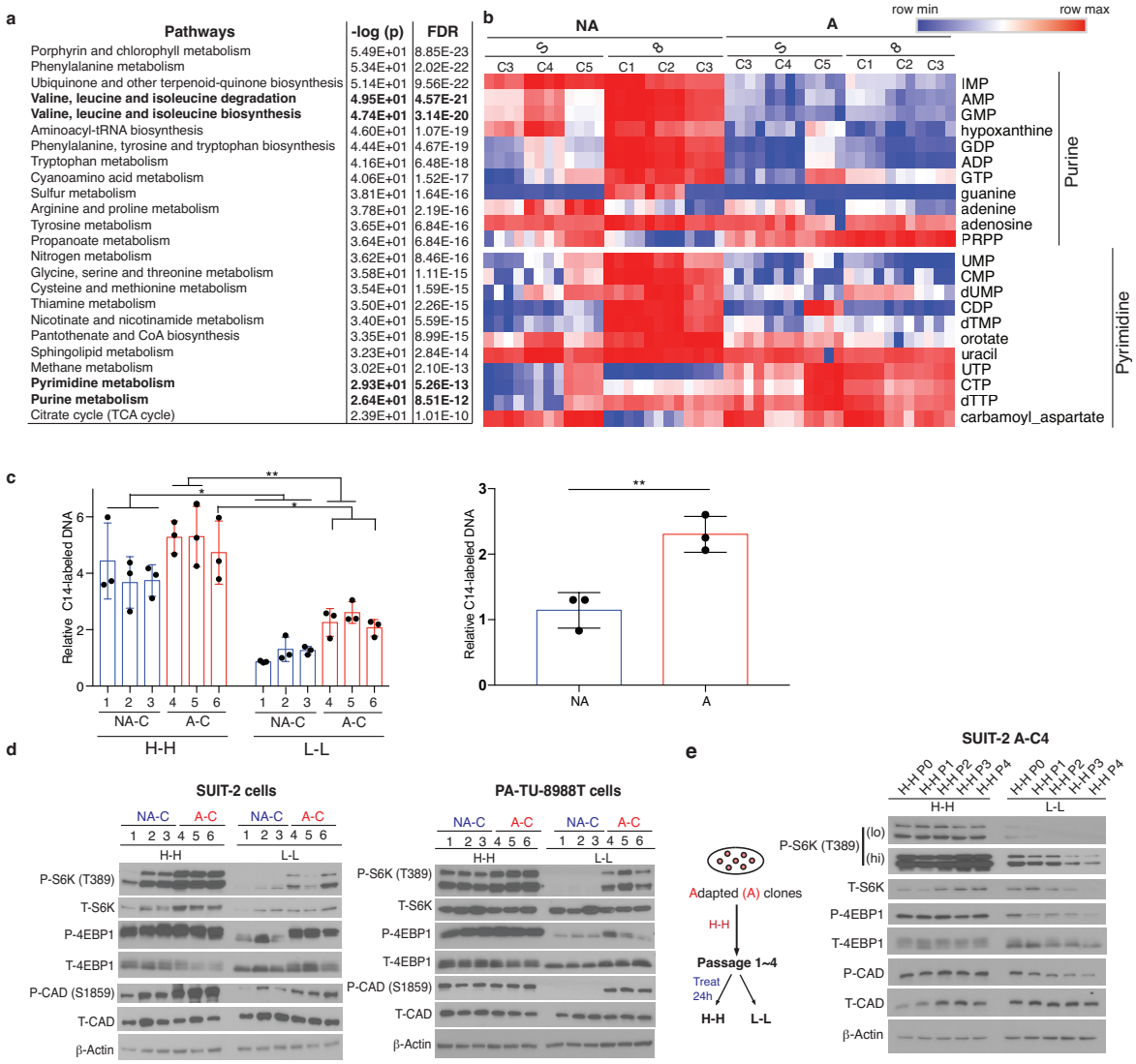

Figure 2.6. Activation of mTORC1 signaling maintains *de novo* pyrimidine synthesis in adapted-clones (A-C) under L-L conditions.

a, List of top 24 metabolic pathways that were significantly altered among 6 of NA-C and 6 of A-C (combined 8988T and SUIT-2) under L-L conditions for 24 hours. Data were processed by Metaboanalyst 4.0 with the pathway analysis module, and the pathways were ranked by –log of

Figure 2.6. (Continued)

the *P*-value. FDR indicates false discovery rate. (n=4 biological replicates per clone, except for A-C6 in 8988T cells where n = 3). In bold are the pathways mentioned in the results. **b**, Heatmap listing metabolites that reached statistical significance ($P < 0.05$ by t-test) among 2 groups (combined 8988T and SUIT-2): 6 NA-C and 6 A-C under L-L conditions for 24 hours. Data were processed by Metaboanalyst 4.0 with the statistical analysis module. Red indicates increased levels, and blue indicates reduced levels within each group (n=4 biological replicates per clone, except for one outlier in A-6 in 8988T, where n=3). **c**, **(left)** Relative incorporation of radiolabeled U-^{14}C-aspartate into DNA synthesis was performed in 3 NA-C and 3 A-C under H-H or L-L conditions for 40 hours in SUIT-2 cell line. The photon numbers expressed as disintegrations per minute (DPM) were normalized to the DNA quantity. This value than presented as a fold change relative to the normalized value from parental SUIT-2 cells under L-L conditions (n=3). **(right)** Average the values from the (left) figure. **d**, Immunoblots of total or phosphorylated S6K (T308), total or phosphorylated 4EBP1 (S65), total or phosphorylated CAD (S1859) in NA-C and A-C (8988T, SUIT-2) under H-H or L-L conditions for 24 hours. **e**, **(left)** A schematic graph depicting the process of reversing SUIT-2 A-C to H-H media, and further sub-culturing them in H-H conditions for 1-4 (P1-P4) passages (3-15 days). These clones that were reversed in H-H conditions were further exposed to H-H or L-L conditions for 24 hours again. **(right)** Immunoblots of total or phosphorylated S6K (T308), total or phosphorylated 4EBP1 (S65), and total or phosphorylated CAD (S1859) in SUIT-2 A-C4 under H-H or L-L conditions for 24 hours.

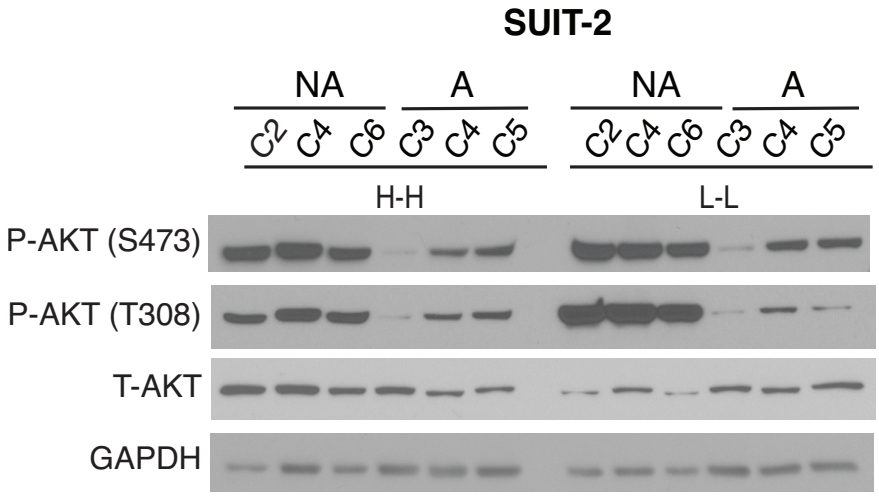

Figure 2.7. Non-adapted clones show increased AKT phosphorylation.

Immunoblots of total or phosphorylated AKT (S473 or T308) in NA-C and A-C (SUIT-2) under H-H or L-L conditions for 24 hours.

Several passages (Fig. 2.6e), and then transiently challenged these clones again with L-L media conditions. This experiment revealed that the longer the adapted clones were maintained in H-H conditions, the more suppression in mTORC1 activity was achieved (reduced p-S6K, p-4EBP1, and p-CAD). Therefore, we concluded that the adapted clones maintained mTORC1 activity under L-L conditions as a result of a metabolic adaptation, independent of genetic mutations, so as to maintain a proliferative phenotype.

2.4.3 Adapted clones display increased GS protein expression and glutamine synthesis activity.

Glutamine is an important nitrogen source for nucleotide synthesis. However, it was supplemented at a very low concentration (0.1 mM) in L-L media compared to 11 mM and 25 mM in RPMI and DMEM media, respectively. Given that several reports demonstrated that deprivation of glutamine transiently enhances glutamine synthesis in some cancer types (*12, 19-22*), we hypothesized that the adapted clones may also have increased glutamine synthesis activity and/or are able to use the limited glutamine more efficiently. Glutamine synthetase (GS), the enzyme required for synthesizing glutamine through catalysis of the ATP-dependent conversion of glutamate and ammonia to glutamine (Fig. 2.8a), was increased at the protein level in adapted clones under L-L conditions in comparison to non-adapted clones (Fig. 2.8b). However, no significant differences were observed at the transcriptional level (Fig. 2.9a,b). Given that GS protein levels were barely detectable under H-H conditions in both clones (Fig. 2.8b), we reasoned that GS protein was regulated differently at the post-transcriptional level between non-adapted clones and adapted clones under L-L conditions. Consistent with the immunoblot data, ^{15}N-NH_4Cl

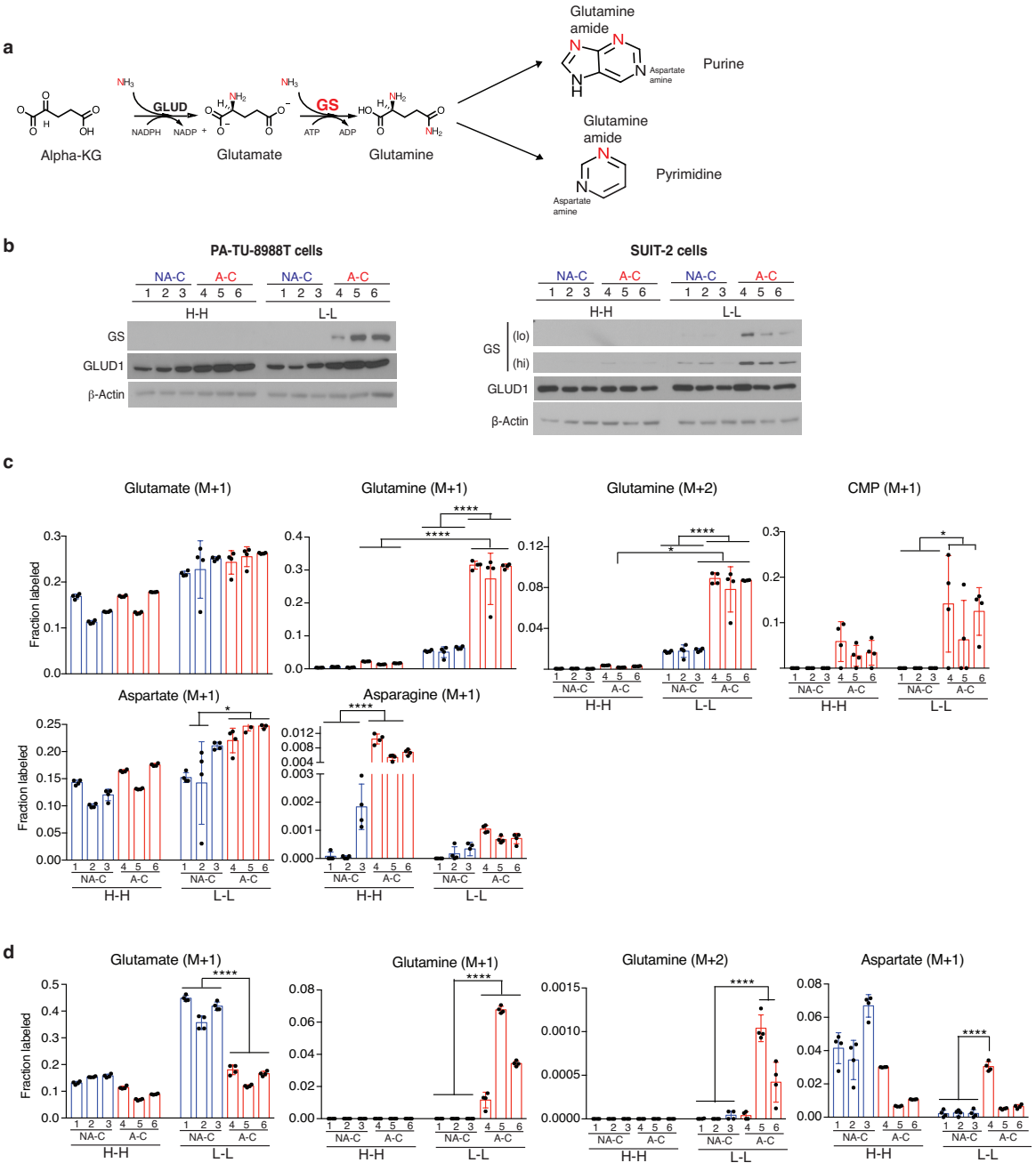

Figure 2.8. Adapted clones display increased glutamine synthesis activity under L-L conditions.

Figure 2.8 (Continued)

a, Pathway illustrates the glutamine synthesis reaction catalyzed by glutamine synthetase (GS) protein. The nitrogen of glutamine (amide) can be incorporated into purine and pyrimidine rings. **b**, Immunoblots of GS protein in NA-C and A-C (8988T, SUIT-2) under H-H or L-L conditions for 24 hours. **c**, Fraction of ^{15}N-labeled metabolites from SUIT-2 clones treated with ^{15}N-NH_4Cl (0.75 mM) tracer in H-H or L-L conditions for 24h (n=4, biological replicates). **d**, Fraction of ^{15}N-labeled metabolites from 8988T clones treated with ^{15}N-glutamic acid (0.1 mM) tracer in H-H or L-L conditions for 24h (n=4, biological replicates).

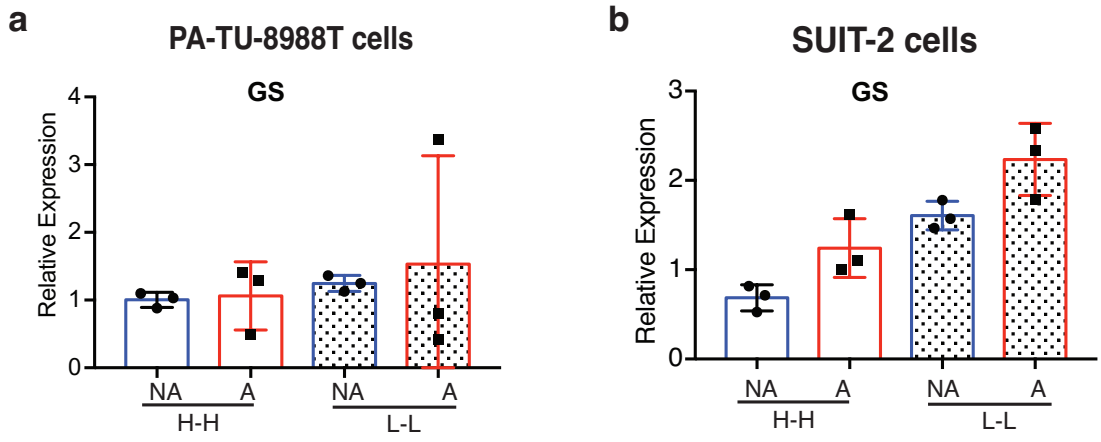

Figure 2.9. Non-adapted clones and adapted clones display similar GS transcriptional levels.

a, Relative gene expression of GS in NA-C and A-C (8988T) under H-H or L-L conditions for 24 hours. **b**, Relative gene expression of GS in NA-C and A-C (SUIT-2) under H-H or L-L conditions for 24 hours.

tracing experiment revealed that adapted clones exhibit enhanced glutamine synthesis activity with an elevated labeled glutamine (M+1, M+2) in comparison to non-adapted clones in L-L conditions (Fig. 2.8c), whereas the labeled glutamine (M+1, M+2) levels were almost undetectable under H-H conditions in both non-adapted clones and adapted clones. This result confirms that the adapted clones have rewired their metabolism under nutrient-limiting conditions. Although we did not see any difference in labeled glutamate (M+1) between non-adapted clones and adapted clones, labeled aspartate (M+1), asparagine (M+1), and pyrimidine species (M+1) were also increased in adapted clones compared to non-adapted clones under L-L conditions. Overall, these data indicate that adapted clones are able to synthesize glutamine, and to provide nitrogen for nucleotide synthesis under L-L conditions.

2.4.4 Adapted clones utilize exogenous amino acids for glutamine synthesis

To investigate the nitrogen sources for glutamine synthesis, we performed ^{15}N-glutamate tracing experiment to delineate a possible source. We demonstrated that adapted clones could utilize exogenous glutamate to synthesize glutamine (M+1, M+2) at a higher level than non-adapted clones in L-L conditions (Fig. 2.8d). Our previous metabolic profiling experiment showed that several amino acids pathways were altered among non-adapted clones and adapted clones, including branch-chain amino acids (BCAA-Leu, Iso, Val) degradation/biosynthesis pathway (Fig. 2.6a). Perhaps, the lower levels of amino acids displayed in adapted clones (Fig. 2.10a) might account for increased utilization by adapted clones (Fig. 2.10b). We then examined whether adapted clones could utilize the nitrogen from branched chain amino acids (BCAAs) for

synthesizing glutamate through BCAA transamination. Immunoblots showed that adapted clones had increased BCAA transaminase 1/2 (BCAT1/2) protein levels (Fig. 2.10c).

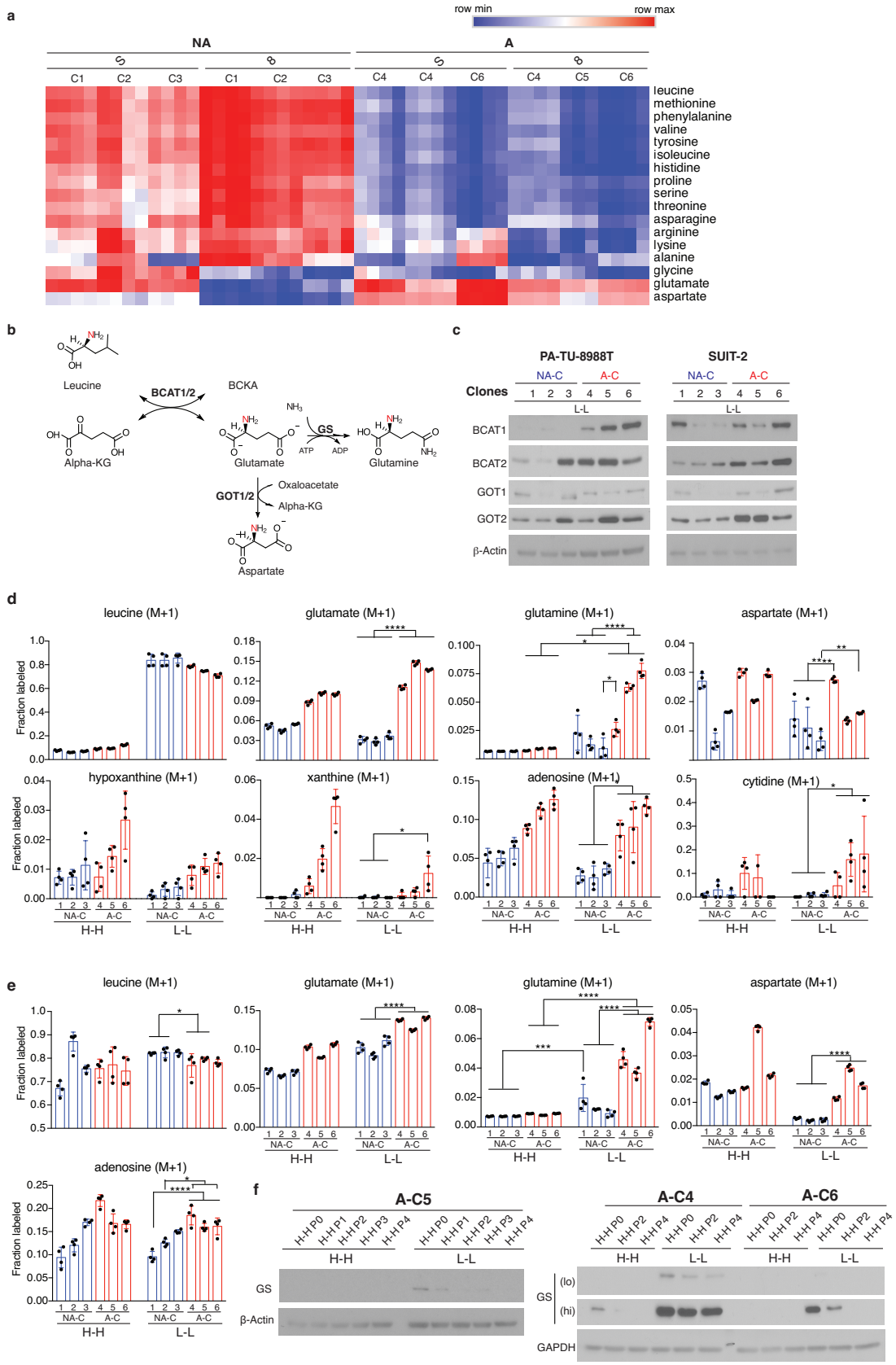
a
row min
row max
NA
A
S
R
C1 C2 C3 C1 C2 C3 C4 C4 C6 C4 C5 C6
leucine
methionine
phenylalanine
valine
tyrosine
isoleucine
histidine
proline
serine
threonine
asparagine
arginine
lysine
alanine
glycine
glutamate
aspartate
b
Leucine
BCAT1/2
BCKA
Alpha-KG
Glutamate
GS
ATP
ADP
Glutamine
GOT1/2
Oxaloacetate
Alpha-KG
Aspartate
c
PA-TU-8988T
SUIT-2
Clones
NA-C
A-C
1 2 3 4 5 6
L-L
BCAT1
BCAT2
GOT1
GOT2
β-Actin
d
leucine (M+1)
glutamate (M+1)
glutamine (M+1)
aspartate (M+1)
hypoxanthine (M+1)
xanthine (M+1)
adenosine (M+1)
cytidine (M+1)
Fraction labeled
H-H
L-L
e
leucine (M+1)
glutamate (M+1)
glutamine (M+1)
aspartate (M+1)
adenosine (M+1)
Fraction labeled
H-H
L-L
f
A-C5
A-C4
A-C6
H-H P0
H-H P1
H-H P2
H-H P3
H-H P4
GS
β-Actin
(lo)
(hi)
GAPDH

Figure 2.10 (Continued)

Adapted clones (A-C) display enhanced leucine incorporation for glutamine synthesis under L-L conditions

a, Heatmap listing amino acids that reached statistical significance ($P < 0.05$ by t-test) among 2 groups (combined 8988T and SUIT-2): 6 NA-C and 6 A-C under L-L conditions for 24h. Data were processed by Metaboanalyst 4.0 with the statistical analysis module. Red indicates increased levels, and blue indicates reduced levels within each group (n=4 biological replicates per clone, except for one outlier in A-6 in 8988T, where n=3). **b**, Pathway illustrates the transamination process from leucine to glutamate through branch-chain-aminotransferase 1/2 (BCAT1/2). **c**, Immunoblots of BCAT1/2 and glutamate-oxaloacetate transferase 1/2 (GOT1/2) in NA-C and A-C (8988T, SUIT-2) under H-H or L-L conditions for 24h. **d**, Fraction of ^{15}N-labeled metabolites from 8988T clones labeled with ^{15}N-leucine (0.4 mM) tracer in H-H or L-L conditions for 24h (n=4, biological replicates). **e**, Fraction of ^{15}N-labeled metabolites from SUIT-2 clones labeled with ^{15}N-leucine (0.4 mM) tracer in H-H or L-L conditions for 24h (n=4, biological replicates). **f**, Immunoblots of GS protein from SUIT-2 A-C that were reversed in H-H conditions for 1-4 passages, and then subjected to H-H or L-L conditions for 24h again.

In alignment with the immunoblot data, ^{15}N-leucine tracing results revealed that adapted clones displayed enhanced fraction labeled ^{15}N-glutamate (M+1), -glutamine (M+1), and -nucleoside base (M+1) under L-L conditioned, compared to non-adapted clones (Fig. 2.10d, e). Interestingly, adapted clones also displayed elevated fraction labeled ^{15}N-aspartate that correlates to the increased glutamic-oxaloacetate transaminase (GOT) 1/2 GOT protein expression in L-L conditions. Taken together, adapted clones could also utilize BCAA as a nitrogen source to synthesize glutamine under nutrient-poor conditions. In line with the reversible mTORC1 signatures that were displayed in the reversed adapted clones (Fig. 2.6e), the increased GS protein levels which were shown in adapted clones were diminished (Fig. 2.10f) when adapted clones were reversed in H-H conditions for several passages.

2.4.5 Activation of mTORC1 signaling stabilizes GS protein in adapted clones

Given that the mTORC1 activity and the elevation of GS protein levels were concomitantly displayed in adapted clones, we hypothesized that mTORC1 could be a potential upstream regulator of GS, or a downstream effector of GS as shown in previous reports (*23-26*). mTORC kinase catalytic inhibitor, Torin 1 abolished GS protein levels in adapted clones, while transcript levels were either increased or unaltered (Fig. 2.11a,b). This indicated that inhibition of mTORC could down-regulate GS at a post-transcriptional level. Most of the clones also showed reduction in GS protein levels upon treatment with mTORC1 selective inhibitor, Rapamycin (data not shown), although mTORC1 signaling was only partially inhibited by Rapamycin as previously shown (*27*). To further examine the mechanism of mTORC1-GS regulation, we treated A-C with a translation inhibitor, cycloheximide (CHX), and demonstrated that GS proteolysis was accelerated by Torin 1 treatment (Fig. 2.11c), suggesting that mTORC1 regulates GS post-

translationally by maintaining GS protein stability under L-L conditions. In addition, GS protein has been shown to be degraded in the proteasome through ubiquitination under high glutamine conditions (*28, 29*). Consistent with these results, the proteasome inhibitor, MG132 induced an increase of GS protein levels in non-adapted clones, however, the GS protein levels in adapted clones were unaltered (Fig. 2.11d). Inhibition of mTORC1 has been shown to enhance proteasomal degradation of long half-life proteins (*30*), although GS protein was not the candidate in that study. MG132 was able to rescue GS protein levels in Torin 1-treated adapted clones (Fig. 2.11e). Furthermore, we confirmed that Torin 1 promoted GS poly-ubiquitination status by performing a co-immunoprecipitation experiment (Fig. 2.11f). Overall, we concluded that activation of mTORC1 activity in A-C under L-L conditions stabilized GS protein, and prevented its degradation in the proteasome as an adapted response in order to synthesize glutamine under nutrient-deprived conditions. Although we do not know how mTORC1 signaling stabilizes GS protein mechanistically, it is possible that the mTORC1 signaling either inhibits ubiquitination, or stimulates de-ubiquitination processes. Nonetheless, we identified a novel downstream target of mTORC1 signaling, which was regulated at a post-translational level by mTORC1.

2.4.6 Adapted clones are sensitive to GS inhibition and are more tumorigenic *in vivo*

To examine if glutamine synthesis is required for adapted clones to proliferate under L-L conditions, we treated adapted clones with the pharmacological inhibitor of GS, Methionine sulfoximide (MSO). We found that adapted clones are sensitive to MSO under L-L, but not under H-H conditions (Fig. 2.12a), mirroring the fact that adapted clones had elevated glutamine synthetase activity only in L-L conditions (Fig. 2.8d, 2.10d,e). In addition, targeting GS with short interfering RNA (siRNA) in adapted clones also lead to a cytostatic effect (Fig. 2.12b, c),

suggesting that glutamine synthesis activity is important for A-C to proliferate under L-L conditions. Lastly, to expand on our *in vitro* finding, we injected both adapted clones and non-adapted clones orthotopically as xenografts. We found that adapted clones were able to form larger tumors compared to non-adapted clones (Fig 2.12d, e). Interestingly, despite the fact that non-adapted clones were also derived from the parental PDAC cell lines, only one mouse formed a tumor.

Taken together, we identified a metabolic adaptation mechanism for PDAC cells to survive under shortage of glucose and glutamine conditions, which reflects certain situations *in vivo*. This involves the ability to utilize amino acids as a source for glutamine synthesis. Beyond the well-known functions of mTORC1(*17*), we identified a new role of mTORC1, in promoting GS protein stability.

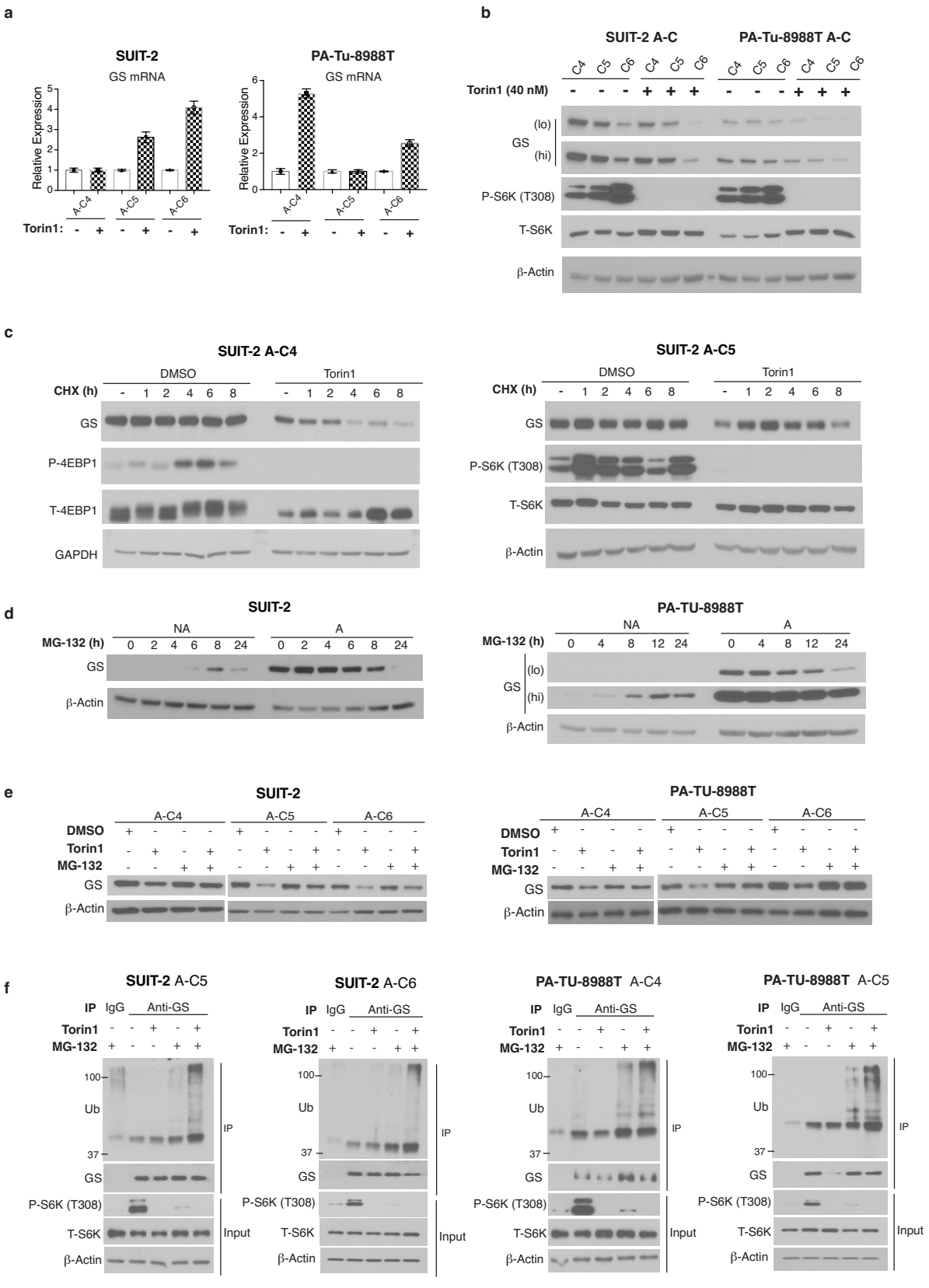
a
SUIT-2
GS mRNA
Relative Expression
A-C4
A-C5
A-C6
Torin1: - + - + - +
PA-Tu-8988T
GS mRNA
Relative Expression
A-C4
A-C5
A-C6
Torin1: - + - + - +
b
SUIT-2 A-C
PA-Tu-8988T A-C
C4 C5 C6 C4 C5 C6
Torin1 (40 nM) - - - + + +
GS
(lo)
(hi)
P-S6K (T308)
T-S6K
β-Actin
c
SUIT-2 A-C4
DMSO
Torin1
CHX (h) - 1 2 4 6 8 - 1 2 4 6 8
GS
P-4EBP1
T-4EBP1
GAPDH
SUIT-2 A-C5
DMSO
Torin1
CHX (h) - 1 2 4 6 8 - 1 2 4 6 8
GS
P-S6K (T308)
T-S6K
β-Actin
d
SUIT-2
NA
A
MG-132 (h) 0 2 4 6 8 24 0 2 4 6 8 24
GS
β-Actin
PA-TU-8988T
NA
A
MG-132 (h) 0 4 8 12 24 0 4 8 12 24
GS
(lo)
(hi)
β-Actin
e
SUIT-2
A-C4
A-C5
A-C6
DMSO + - - - + - - - + - - -
Torin1 - + - + - + - + - + - +
MG-132 - - + + - - + + - - + +
GS
β-Actin
PA-TU-8988T
A-C4
A-C5
A-C6
DMSO + - - - + - - - + - - -
Torin1 - + - + - + - + - + - +
MG-132 - - + + - - + + - - + +
GS
β-Actin
f
SUIT-2 A-C5
IP IgG Anti-GS
Torin1 - - + - +
MG-132 + - - + +
100
Ub
37
GS
P-S6K (T308)
T-S6K
β-Actin
IP
Input
SUIT-2 A-C6
IP IgG Anti-GS
Torin1 - - + - +
MG-132 + - - + +
100
Ub
37
GS
P-S6K (T308)
T-S6K
β-Actin
IP
Input
PA-TU-8988T A-C4
IP IgG Anti-GS
Torin1 - - + - +
MG-132 + - - + +
100
Ub
37
GS
P-S6K (T308)
T-S6K
β-Actin
IP
Input
PA-TU-8988T A-C5
IP IgG Anti-GS
Torin1 - - + - +
MG-132 + - - + +
100
Ub
37
GS
P-S6K (T308)
T-S6K
β-Actin
IP
Input

Figure 2.11 (Continued)

mTORC1 inhibition promote GS protein degradation through ubiquitin-proteasome system.

a, Relative gene expression of GS under DMSO control or Torin 1 (40 nM) treatment for 24h in SUIT-2 or 8988T A-C under L-L conditions. Data indicate the mean ± SD. **b**, Immunoblots of GS and total or phosphorylated S6K (T308) in A-C (8988T, SUIT-2) under L-L conditions along with DMSO control or Torin 1 (40 nM) treatment for 24h. **c**, Immunoblots of GS, total or phosphorylated 4EBP1, total or phosphorylated S6K (T308) in A-C (8988T, SUIT-2) under L-L conditions along with DMSO control or Torin 1 (200 nM) treatment for 8h, combining translation inhibitor, cycloheximide (CHX) (20 μg/ml) added at the indicated time points. **d**, Immunoblots of GS in NA-C or A-C (8988T, SUIT-2) under L-L conditions upon treatment with the proteasome inhibitor, MG132 (0.5 μM) at the indicated time points. **e**, Immunoblots of GS in A-C (8988T, SUIT-2) under L-L conditions with Torin1 (200 nM) alone, MG-132 (10 μM) alone, or in combination for 6 or 8 hours. **f**, Immunoblots of ubiquitination status in A-C (8988T, SUIT-2) following co-immunoprecipitation experiments with GS antibody in the same conditions as shown in (**e**). Endogenous GS and total or phosphorylated S6K (T308) proteins are also shown here.

2.5 Discussion

Metabolic plasticity in cancer has been addressed in many studies regarding how cancer cells cope with versatile nutrient availability (*1, 12, 19, 28, 31-33*). However, the caveat of understanding cancer metabolism when utilizing the commercial culture media is that *in vitro* media contains supraphysiological levels of nutrients, which might not reflect how tumors respond *in vivo* (*34, 35*). PDAC cells are known to require exogenous glucose and glutamine for nucleotide synthesis and balancing redox levels, respectively (*2, 4*), however, both glucose and glutamine can be depleted *in vivo (1)*.

To understand how PDAC cells can manage to overcome these harsh conditions, we selected PDAC clonal cells that were able to adapt and be sub-cultured in limited-glucose and glutamine media. In contrast to the studies that have shown the dependency on exogenous glucose and glutamine in PDAC cells (*2*), we revealed that some clonal cells can adapt in the harsh conditions. These clones maintained mTORC1 activation, which not only promoted nucleotide synthesis but also enhanced glutamine synthesis by stabilizing GS protein. In our findings, we identified a novel target upon mTOR inhibition through the ubiquitin proteasome system (UPS) (*30*). Yet, how adapted clones sustain mTORC1 activation under this nutrient-deprived condition remains to be determined. Deprivation of leucine alone reduced mTORC1 signaling in adapted clones, although the activity is not fully abolished (discussed in chapter 3), suggesting that exogenous leucine might play a partial role in mTORC1 activation. On the other hand, asparagine present in the DMEM media has been shown to induce GS protein level under glutamine deprivation (*9*). However, we observed reduced mTORC1 activity, but enhanced GS protein when asparagine was present in the media. This contradicts what we observed for

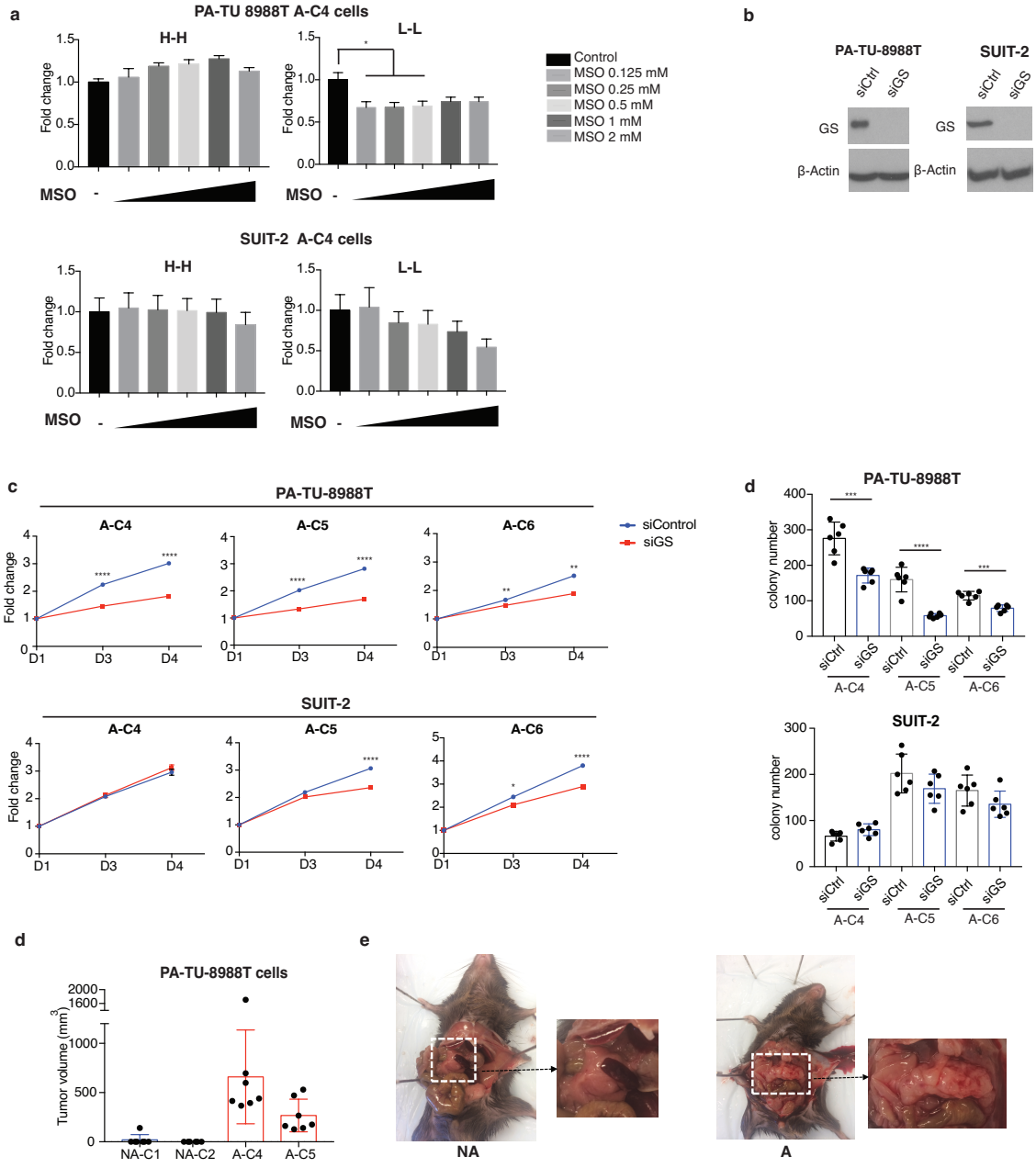

Figure 2.12. Adapted clones are sensitized to inhibition of GS, and exhibit enhanced tumorigenesis *in vivo*.

a, Cell numbers were measured by the Celigo machine (Nexcelom Bioscience) upon GS inhibitor, Methionine sulfoximine (MSO) treatment for 72h under H-H or L-L conditions with

Figure 2.12 (Continued)

indicated concentrations. The numbers are presented as fold changes relative to the numbers at day (n=6) 1. **b**, Verification of GS protein with short interfering (si) RNA against GS or negative control after 24h post-transfection in A-C (8988T, SUIT-2) under L-L conditions. **c**, Proliferation curves of A-C (8988T, SUIT-2) upon siGS transfection validated from (**b**) under L-L conditions for 4 days. Data are shown as mean ± SEM; *$P < 0.05$; **$P < 0.01$; ***$P < 0.001$; ****$P < 0.0001$. **d**, Tumor volume of NA-C and A-C at 33 days following orthotopical injection of 8988T cells into the pancreas of immunodeficient mice. **e**, Representative pictures of the tumors from NA-C and A-C xenografts described in (**d**).

mTORC1-GS regulation (discussed in the chapter 3), suggesting that the regulation of GS might be different under different contexts.

We identified a role of glutamine synthesis activity when cells are grown under nutrient-deprived conditions, suggesting that targeting glutamine synthesis might be a potential strategy for treating PDAC or treating in combination with current drugs.

2.6 Reference

1. J. J. Kamphorst *et al.*, Human pancreatic cancer tumors are nutrient poor and tumor cells actively scavenge extracellular protein. *Cancer research* **75**, 544-553 (2015).

2. J. Son *et al.*, Glutamine supports pancreatic cancer growth through a KRAS-regulated metabolic pathway. *Nature* **496**, 101 (2013).

3. D. Gaglio *et al.*, Oncogenic K-Ras decouples glucose and glutamine metabolism to support cancer cell growth. *Molecular systems biology* **7**, 523 (2011).

4. H. Ying *et al.*, Oncogenic Kras maintains pancreatic tumors through regulation of anabolic glucose metabolism. *Cell* **149**, 656-670 (2012).

5. S. Yang *et al.*, Pancreatic cancers require autophagy for tumor growth. *Genes & development*, (2011).

6. A. Yang *et al.*, Autophagy is critical for pancreatic tumor growth and progression in tumors with p53 alterations. *Cancer discovery*, (2014).

7. R. M. Perera *et al.*, Transcriptional control of autophagy–lysosome function drives pancreatic cancer metabolism. *Nature* **524**, 361 (2015).

8. C. Commisso *et al.*, Macropinocytosis of protein is an amino acid supply route in Ras-transformed cells. *Nature* **497**, 633 (2013).

9. N. N. Pavlova *et al.*, As extracellular glutamine levels decline, asparagine becomes an essential amino acid. *Cell metabolism* **27**, 428-438. e425 (2018).

10. L. B. Sullivan *et al.*, Aspartate is an endogenous metabolic limitation for tumour growth. *Nature cell biology* **20**, 782 (2018).

11. J. Garcia-Bermudez *et al.*, Aspartate is a limiting metabolite for cancer cell proliferation under hypoxia and in tumours. *Nature cell biology* **20**, 775 (2018).

12. M. Tajan *et al.*, A role for p53 in the adaptation to glutamine starvation through the expression of SLC1A3. *Cell metabolism* **28**, 721-736. e726 (2018).

13. M. Pan *et al.*, Regional glutamine deficiency in tumours promotes dedifferentiation through inhibition of histone demethylation. *Nature cell biology* **18**, 1090 (2016).

14. J. L. Yecies *et al.*, Akt stimulates hepatic SREBP1c and lipogenesis through parallel mTORC1-dependent and independent pathways. *Cell metabolism* **14**, 21-32 (2011).

15. A. M. Robitaille *et al.*, Quantitative phosphoproteomics reveal mTORC1 activates de novo pyrimidine synthesis. *Science* **339**, 1320-1323 (2013).

16. I. Ben-Sahra, G. Hoxhaj, S. J. Ricoult, J. M. Asara, B. D. Manning, mTORC1 induces purine synthesis through control of the mitochondrial tetrahydrofolate cycle. *Science* **351**, 728-733 (2016).

17. A. J. Valvezan, B. D. Manning, Molecular logic of mTORC1 signalling as a metabolic rheostat. *Nature Metabolism*, 1 (2019).

18. I. Ben-Sahra, J. J. Howell, J. M. Asara, B. D. Manning, Stimulation of de novo pyrimidine synthesis by growth signaling through mTOR and S6K1. *Science*, 1228792 (2013).

19. S. Tardito *et al.*, Glutamine synthetase activity fuels nucleotide biosynthesis and supports growth of glutamine-restricted glioblastoma. *Nature cell biology* **17**, 1556 (2015).

20. A. J. Bott *et al.*, Oncogenic Myc induces expression of glutamine synthetase through promoter demethylation. *Cell metabolism* **22**, 1068-1077 (2015).

21. S. Loeppen *et al.*, Overexpression of glutamine synthetase is associated with β-catenin-mutations in mouse liver tumors during promotion of hepatocarcinogenesis by phenobarbital. *Cancer research* **62**, 5685-5688 (2002).

22. S. H. Issaq, A. Mendoza, S. D. Fox, L. J. Helman, Glutamine synthetase is necessary for sarcoma adaptation to glutamine deprivation and tumor growth. *Oncogenesis* **8**, 20 (2019).

23. H. W. S. Tan, A. Y. L. Sim, Y. C. Long, Glutamine metabolism regulates autophagy-dependent mTORC1 reactivation during amino acid starvation. *Nature communications* **8**, 338 (2017).

24. A. O. A. Michael *et al.*, Inhibiting Glutamine-Dependent mTORC1 Activation Ameliorates Liver Cancers Driven by β-Catenin Mutations. *Cell Metabolism*, (2019).

25. J. L. Jewell *et al.*, Differential regulation of mTORC1 by leucine and glutamine. *Science* **347**, 194-198 (2015).

26. E. Bernfeld *et al.*, Phospholipase D–dependent mTOR complex 1 (mTORC1) activation by glutamine. *Journal of Biological Chemistry* **293**, 16390-16401 (2018).

27. A. Y. Choo, S.-O. Yoon, S. G. Kim, P. P. Roux, J. Blenis, Rapamycin differentially inhibits S6Ks and 4E-BP1 to mediate cell-type-specific repression of mRNA translation. *Proceedings of the National Academy of Sciences* **105**, 17414-17419 (2008).

28. T. V. Nguyen *et al.*, Glutamine Triggers Acetylation-Dependent Degradation of Glutamine Synthetase via the Thalidomide Receptor Cereblon. *Mol Cell* **61**, 809-820 (2016).

29. T. V. Nguyen *et al.*, p97/VCP promotes degradation of CRBN substrate glutamine synthetase and neosubstrates. *Proc Natl Acad Sci U S A* **114**, 3565-3571 (2017).

30. J. Zhao, B. Zhai, S. P. Gygi, A. L. Goldberg, mTOR inhibition activates overall protein degradation by the ubiquitin proteasome system as well as by autophagy. *Proceedings of the National Academy of Sciences* **112**, 15790-15797 (2015).

31. K. Birsoy *et al.*, Metabolic determinants of cancer cell sensitivity to glucose limitation and biguanides. *Nature* **508**, 108 (2014).

32. G. Arad, A. Freikopf, R. G. Kulka, Glutamine-stimulated modification and degradation of glutamine synthetase in hepatoma tissue culture cells. *Cell* **8**, 95-101 (1976).

33. X. H. Lowman *et al.*, p53 Promotes Cancer Cell Adaptation to Glutamine Deprivation by Upregulating Slc7a3 to Increase Arginine Uptake. *Cell Reports* **26**, 3051-3060. e3054 (2019).

34. J. R. Cantor *et al.*, Physiologic medium rewires cellular metabolism and reveals uric acid as an endogenous inhibitor of UMP synthase. *Cell* **169**, 258-272. e217 (2017).

35. J. V. Voorde *et al.*, Improving the metabolic fidelity of cancer models with a physiological cell culture medium. *Science advances* **5**, eaau7314 (2019).

Chapter 3:

Discussion and future directions

3.1 Overview

In this dissertation, I have identified one of the metabolic adaptation responses under (glutamine-limiting conditions. Using PDAC cells that were adapted to these harsh conditions, I demonstrated that these cells acquire mTORC1 activity even under starvation conditions, which in turn increased nucleotide synthesis and stabilized the glutamine synthetase (GS) protein (Fig. 3.1). Targeting glutamine synthesis pathway rendered the cells susceptible to low glucose-low glutamine conditions *in vitro*, highlighting the importance of targeting GS as a therapeutic target, when tumors reside in a nutrient-poor environment. In this chapter, I demonstrate the implications from my findings, share unpublished data, and discuss future directions for unanswered questions.

3.2 What signals activate mTORC1 signaling in adapted clones under nutrient starvation conditions?

There are two well-characterized branches to activate mTORC1 signaling, which are either through growth factors or through amino acids inputs (*1*). The growth factors activate mTORC1 activity by releasing the Tuberous Sclerosis Complex (TSC) complex, a negative regulator from Rheb protein, which is an essential activator for mTORC1. Moreover, phosphorylation of TSC by AKT suppresses the interaction of TSC with Rheb. In my findings, while non-adapted clones exhibit AKT activity with phosphorylation at T308 (target of PDK1) and S473(target of mTORC2), mTORC1 signaling was completely abolished under L-L conditions. Therefore, I deduced that the amino acids arm to activate mTORC1 might be suppressed in non-adapted

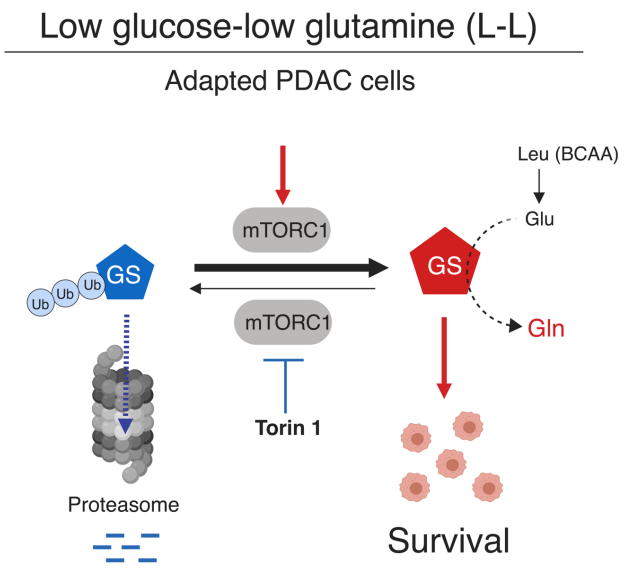

Figure 3.1. Schematic model of the adaptation mechanism of PDAC cells that survive in the low glucose-low glutamine (L-L) conditions.

PDAC cells maintain activation of mTORC1 signaling which enhances glutamine synthetase (GS) protein stability as an adaptive response to survive under low glucose and low glutamine conditions. The cells utilize the nitrogen from amino acids (Leu, Glu) for synthesizing glutamine to maintain nucleotide pools for proliferation under these harsh conditions. On the other hand, inhibition of mTORC by Torin 1 promotes GS proteolysis by the proteasome.

clones, or the upregulation of AKT activity in non-adapted clones was due to a negative feedback regulation of mTORC1 (*2*).

Deprivation of leucine alone in the adapted clones reduced mTORC1 signaling with decreased protein levels of phosphorylation of S6K, although the activity was not fully abolished (Fig 3.2a). Along with suppressed mTORC1 activity by leucine deprivation, GS protein was also reduced, confirming our mTORC1-GS axis regulation. The results indicated that exogenous leucine plays an important role in the activation of mTORC1 activity in the adapted clones. Although several reports indicated that leucine alone is an important activator for mTORC1 along with the presence of growth factors, the reason for non-adapted clones not responding to exogenous leucine under L-L conditions remains to be explored. In addition, the adapted clones displayed an increase in the protein level of L-type amino acid transporter 1 (LAT1; also known asSLC7A5) (Fig. 3.2b), which is important for the influx of large neutral amino acids, including leucine. Whether adapted clones exhibit increased leucine uptake, which is required for activation of mTORC1 activity, needs future studies to validate it by performing radio-isotope experiment. Moreover, this hypothesis is consistent with what Bott *et al*. (*3*) have shown, namely that overexpression of GS in the breast cancer cell Hs578T is sufficient to increase leucine uptake in an L-type amino acid transporter-dependent manner. To rule out whether there is an association between GS levels and leucine uptake, we can perform a leucine uptake assay while inhibiting GS. In addition, leucine deprivation not only suppressed mTORC1 activity in adapted clones, but also inhibited cell proliferation under L-L conditions (Fig. 3.2c). This inhibition effect was more dramatic when adapted clones were deprived of all branch-chain amino acids (BCAA: Leu, Iso, Val). Overall, my findings showed that the role of leucine not only can be used as a source for

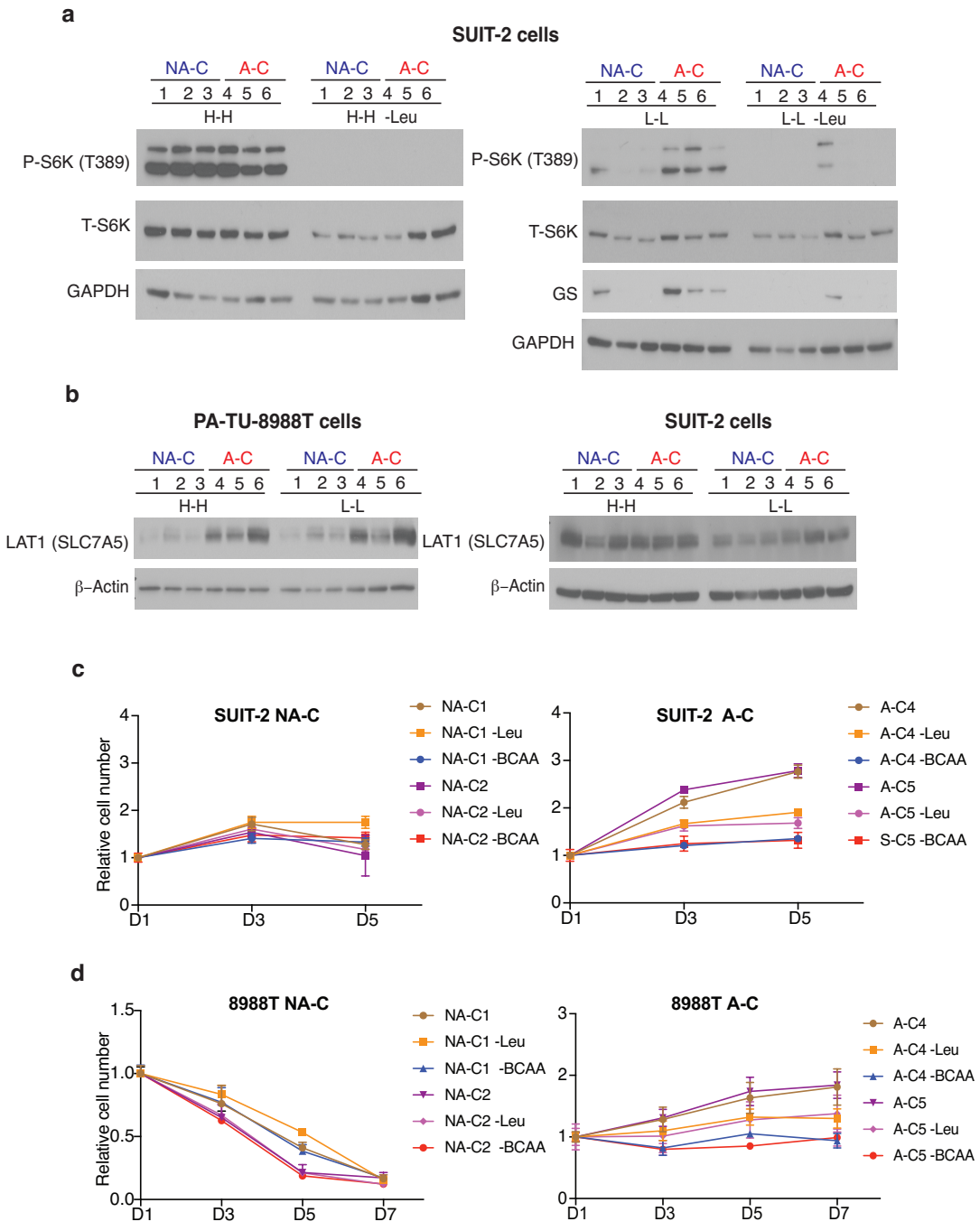

Figure 3.2. Leucine deprivation reduced mTORC1 activity and inhibited proliferation in adapted clones.

Fig. 3.2 (Continued)

a, Immunoblots of GS and total or phosphorylated S6K (T308) in A-C (SUIT-2) under H-H or L-L conditions along with leucine deprivation for 24 hours. **b**, Immunoblots of SLC7A5 in NA-C or A-C (8988T, SUIT-2) under H-H or L-L conditions for 24 hours. **c,d**, Proliferation curves of NA-C or A-C (8988T, SUIT-2) in L-L conditions upon leucine deprivation or branch-chain amino acids (Leu, Iso, Val) deprivation for 5 or 7 days. Cell numbers were measured by Celigo machine (Nexcelom Bioscience), and the numbers are presented as a fold change that is relative to day 1 (n=6).

synthesizing glutamine, but it can also activate mTORC1 signaling, which in turn further promotes glutamine synthesis by stabilizing GS protein.

3.3 Is the induction of GS protein expression an universal adaptive mechanism when cells are under a nutrient-deprived environment, specifically in a limited-glutamine condition?

Several reports claimed that deprivation of glutamine drives glutamine synthesis activity either at a transcriptional or a translational level. For instance, Tardito *et al*. (*4*) noted that upon glutamine (Gln) starvation, increased GS protein expression and activity confers Gln prototrophy in glioblastoma (GBM) cells, and that the nitrogen provided from glutamine fuels *de novo* purine synthesis. Injecting $^{13}C_6$-glucose to the patients with GBM, most of the tumors were enriched in glucose-derived ^{13}C-Gln, suggesting that the Gln pool in the tumor is synthesized *in situ*; Bott *et al.* (*3*) demonstrated that breast cancer cells that harbor overexpression of GS can synthesize glutamine in glutamine-deprived media, by performing a ^{15}N-NH_4Cl tracing experiment *in vitro*. In their results, the labeled nitrogen from glutamine can also be incorporated into purine and pyrimidine metabolites. Mechanistically, they identified oncogenic Myc as the driver for the elevated GS gene expression through promoter demethylation; Tajan *et al. (5)* showed that tumor suppressor p53 induces SLC1A3 expression, which is an aspartate/glutamate transporter, allowing colon cancer cells to utilize aspartate to support cell growth in the absence of extracellular glutamine; Nguyen *et al*. (*6*) demonstrated that glutamine starvation induced GS protein expression in myeloma, breast, and lung cancer cell lines, whereas glutamine alone induced degradation of GS. They proposed a model that shows that in the presence of glutamine, p300/CPB proteins acetylate GS at lysines 11 and 14 to create a degron that binds CRBN. Acetylated GS bound to CRBN is ubiquitylated and subsequently degraded by the proteasome.

In my findings (Fig.3.3a), of all the PDAC cell lines that I tested, GS protein levels were induced under L-L conditions as opposed to the levels in H-H conditions. This implied that the elevation of GS expression could be a universal phenomenon in PDAC as well as other cancer types when cells are under a glutamine-deprived conditions as an adaptive mechanism to re-synthesize glutamine. Several functions of GS have been addressed, including the role of GS in detoxifying ammonia in the liver and in protecting neurons against excitotoxicity by converting glutamate into glutamine in the brain. Here, we conclude that the function of GS in nutrient-starved cancer cells is to synthesize glutamine, which can promote cell proliferation under a glucose- and glutamine-deprived conditions.

In an *ex vivo* experiment (Fig. 3.3b) tracing PDAC tumors derived from a genetically engineered mouse (GEMM) model with ^{15}N-NH_4Cl, tumors displayed 3~5 % of labeled-glutamine (M+1, M+2) independent of the glutamine levels present in the media, indicating that glutamine synthesis might be activated in PDAC tumors. Given that tumors might synthesize glutamine *in vivo* through GS, I have not yet provided any direct evidence to show whether GS is required for tumor formation. To examine this hypothesis, I am currently preparing cells that harbor an inducible knockdown shGS construct for an *in vivo* orthotopic experiment. This finding will allow us to elucidate whether GS is essential for tumor progression and whether it could be a potential target to inhibit PDAC growth.

Tissue microarray (TMA) analysis showed that GS protein expression varies between human PDAC patients (n=127) (Fig. 3.3c), However, GS expression did not predict patient median survival (data not shown), which is consistent to what Tardido *et al. (4)* showed in

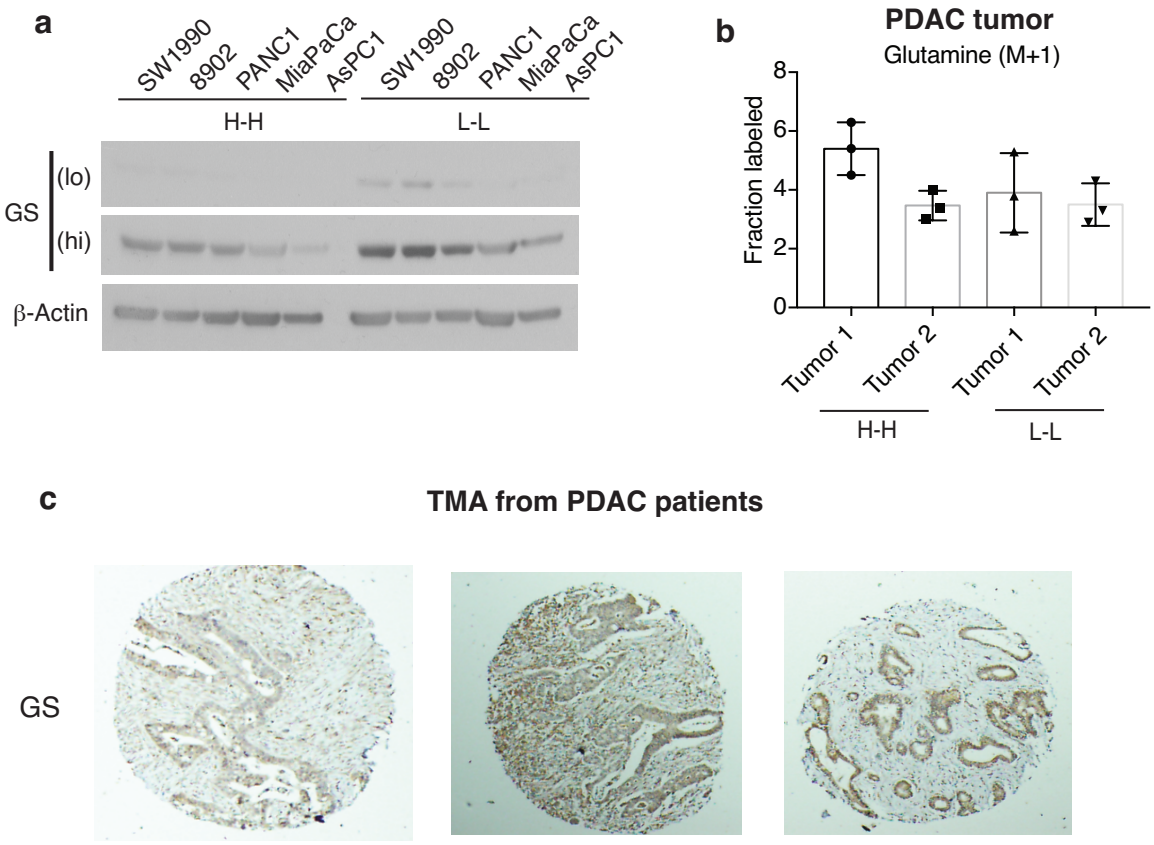

Figure 3.3. GS protein is expressed in PDAC patients and mouse.

a, Immunoblots of GS in human PDAC cell lines treated in H-H or L-L conditions for 24 hours. **b**, Fraction of ^{15}N-labeled glutamine from PDAC tumors derived from a GEMM mouse and subjected to H-H or L-L conditions along with ^{15}N-NH_4Cl (0.75 mM) tracer for 6 hours. (n=3 in each tumor). **c**, Representative pictures of GS protein expression from PDAC patients.

glioblastoma patients. In addition, GS expression is not associated with tumor size, tumor grade, and lymph node numbers (data not shown). It is highly possible that, within the same tumor, GS is expressed in a heterogenous manner among different cells, or that the expression level is dependent on the nutrient level in the regional tumor microenvironment. For instance, the core of tumors is thought to be glutamine-deprived (*7*), and this might affect the expression of GS within the same tumor. Nevertheless, it is still worthwhile to know that tumors express GS protein with the implication that the "glutamine addiction" character from *in vitro* findings (*8*) could be displayed differently *in vivo*, since several results showed that PDAC cells cannot proliferate without exogenous glutamine based on *in vitro* system. It is also possible that there is a cross-talk between cells that express different levels of GS expression. For instance, for those cancer cells that can synthesize glutamine, glutamine can be delivered to the neighboring cancer cells or other types of cells (fibroblast, immune cells, *etc*.). However, this hypothesis will require further studies to be fully addressed.

3.4 What are the potential mechanisms for mTORC1-GS regulation?

In my findings, we have not yet proved whether mTORC1 signaling directly or indirectly regulates GS protein stability. mTORC1 is a serine/threonine kinase protein and has several downstream phospho-targets that have been identified by mass spectrometry (*9*). While GS protein was not a downstream candidate of mTORC1 signaling under a growth factor treatment in their study, several phosphorylation sites have been reported (PhosphoSitePlus website). Nevertheless, when adapted clones were treated under H-H conditions, even in the presence of mTORC1 activity, GS protein was not expressed (Fig. 2.6d). This implies that other proteins are required to orchestrate GS stability in adapted clones under L-L conditions.

In addition, GS acetylated by p300/CPB proteins has been shown to bind to E3 ligase Cereblon (CRBN), and GS protein can get further ubiquitylated and degraded in the proteasome (*6*). In our case, when adapted clones were treated with histone deacetylase (HDAC) inhibitor, Trichostatin A (TSA) or sirtuins inhibitor, nicotinamide (NAM) under L-L conditions, GS protein was suppressed (Fig. 3.4). Combining both inhibitors even showed an additive effect to reduce GS protein expression, suggesting that mTORC1 might potentially activate deacetylases or inhibit acetylases to prevent GS protein from degrading in adapted clones. To examine whether mTORC1 signaling affects post-translational modification on GS, we will first need to pull-down GS by performing the Co-Immunoprecipitation experiment coupled with mass spectroscopy to identify which post-translational modification site might be affected by mTORC1 inhibition. Moreover, we will have to identify potential target proteins that can interact with GS. However, the interaction would be disrupted during Torin 1 treatment. On the other hand, Torin 1 promoting GS degradation through mTORC1 mechanism might be a general proteolysis phenomenon.

Indeed, Zhao *et al*. (*10*) demonstrated that the inhibition of mTORC1 enhances overall protein degradation, specifically in long half-life proteins, by the ubiquitin proteasome system. Although they did not identify GS as a potential target for proteasome degradation through mTORC1 inhibition, my results revealed that HMG-CoA synthase 1 protein levels was also suppressed in adapted clones in addition to GS protein under Torin1 treatment (data not shown). This finding raises a possibility that the degradation of GS protein in adapted clones under Torin 1 treatment might be a global proteolysis effect.

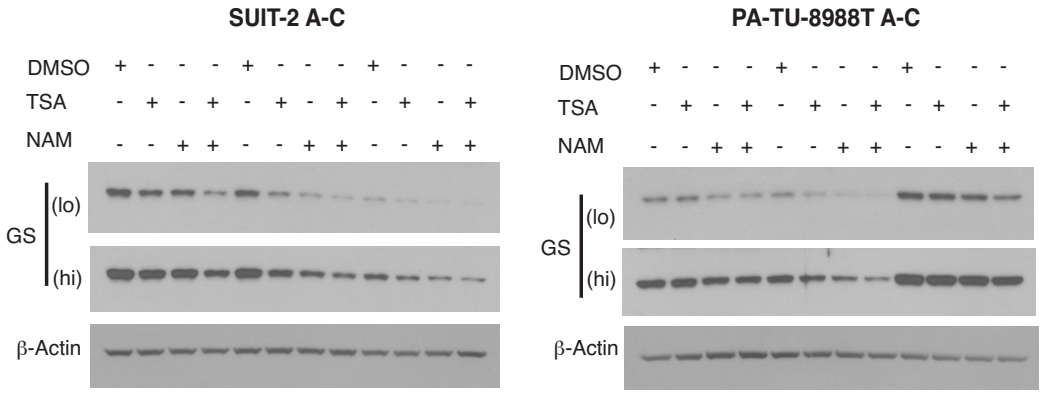

Figure 3.4. Deacetylation inhibitor can reduce GS protein in adapted clones under L-L condition.

Immunoblots of GS in A-C (SUIT-2, 8988T) under L-L conditions for 8 hours along with histone deacetylase (HDAC) inhibitor, Trichostatin A (TSA) or sirtuins inhibitor, nicotinamide (NAM) under L-L conditions.

3.5 Does asparagine present in the media contribute to the induction of GS protein expression?

In a previous report, Pavlova *et al*. (*11*) revealed that when extracellular glutamine levels decline, tumor cells become reliant on exogenous asparagine (ASN) for proliferation and protein synthesis. Asparagine was further shown to stimulate the protein expression of GS, and to promote protein synthesis that concomitantly activates mTORC1 signaling. Although they conducted the experiment in DMEM media, in which the asparagine level is different from the RPMI media that I used, I wanted to confirm whether asparagine could induce GS protein in adapted clones. By treating adapted clones with either no ASN, 0.1 mM of ASN (the same concentration that is present in the DMEM), or 0.4 mM of ASN (the same concentration that is present in the RPMI), I found that although asparagine alone can induce GS expression in a dose-dependent manner, mTORC1 activity was reduced under 0.4 mM of ASN treatment compared to its activity when cells were under 0.1 mM (Fig. 3.5). This finding indicates that asparagine contributes to the partial induction of GS that is independent of mTORC1 signaling in adapted clones under L-L conditions.

3.6 What are the other potential adapted mechanisms in adapted clones that can survive in the L-L conditions?

So far, my thesis project has only focused on the role of glutamine synthesis when PDAC cells are under low glucose and low glutamine conditions. However, several metabolic pathways were altered at the same time, and they might all contribute to the overall survival advantage that is present in adapted clones. Interestingly, while non-adapted clones in both SUIT-2 and 8988T present heterogenous transcriptome signatures from a RNA-seq analysis, the transcriptome

expression in adapted clones among SUIT-2 and 8988T cells were clustered together in the principal component analysis (Fig 3.6), indicating that adapted clones have common rewiring responses that are regulated at the transcriptional level.

To investigate pathway alterations among adapted and non-adapted clones under L-L conditions in our RNA-seq data, we identified several pathways that were enriched in adapted clones besides the nucleotide pathway (purine and pyrimidine metabolism) and the branch-chain amino acids (BCAA) pathway. These enriched pathways include "KEGG_Glycolysis Gluconeogenesis*",* "KEGG_Pentose_Phosphate_Pathway", and "KEGG_Fatty_Acid_Metabolism", *etc* (Fig. 3.7). These three pathways are important given that glucose is an important carbon resource for cellular anabolism, including incorporation into nucleotide synthesis through pentose-phosphate-pathway. However, adapted clones were maintained in limited-glucose media. Within the KEGG_Glycolysis Gluconeogenesis pathway (Fig. 3.8) and the KEGG_Pentose_Phosphate_Pathway (Fig 3.9), the rate-limiting enzyme Phosphoenolpyruvate carboxykinase (PCK) 1 in gluconeogenesis pathway and Phosphoribosyl pyrophosphate synthetase (PRPS) 1/2 in pentose phosphate pathway are induced in adapted clones. Three possibilities can account for the enrichment in these genes: One, adapted clones were able to use the limited-glucose more efficiently compared to non-adapted clones by induced gene expression to support the proliferative demands. Two, adapted clones can utilize other glucogenic amino acids for synthesizing the intermediate metabolites within these pathways. Lastly, both possibilities can occur at the same time, so adapted clones can maximize benefits from the limited resource glucose.

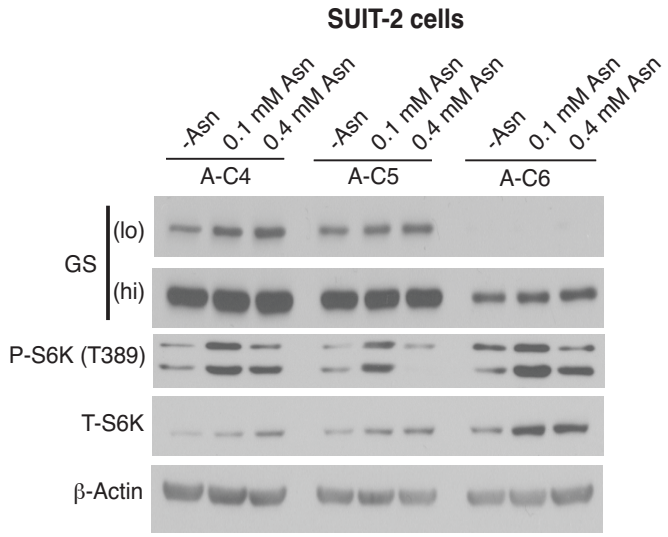

Figure 3.5. Asparagine can increase GS protein expression but the regulation may not be through mTORC1 activity.

Immunoblots of GS and total or phosphorylated S6K (T308) in A-C (SUIT2) under L-L conditions along with either deprivation of asparagine (ASN), supplementation of 0.1 mM ASN or 0.4 mM of ASN.

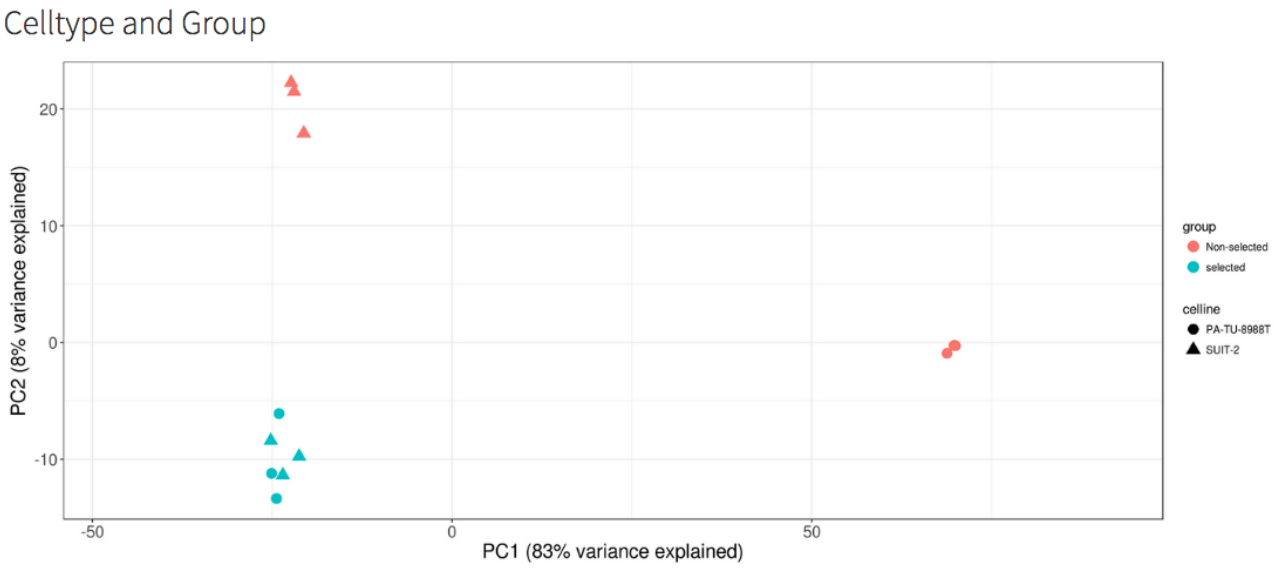

Figure 3.6. Principal component analysis showed the transcriptome of A-C were clustered together under L-L conditions.

Among the 500 most variable genes with NA-C and A-C under L-L conditions for 24 hours, 83% of the variance was segregated in non-selected clones (or NA-C) between SUIT-2 and 8988T cells based on principal component (PC) 1 from a RNA-Seq experiment. Within the selected clones (or A-C), no observed segregation was appeared in PC1 between SUIT-2 and 8988T. Each dot represents a clone.

In fatty acid metabolism (Fig. 3.10), the rate-limiting enzyme in fatty acid oxidation, carnitine palmitoyltransferase (CPT) 1/2 are induced in adapted clones. There is a possibility that adapted clones utilize fatty acid oxidation for maintaining the metabolite pool in the TCA cycle and for further synthesizing glutamate for glutamine synthesis. Consistent with the result from Biancur *et al*. (*12*), they hypothesized that one of the mechanisms of PDAC tumors that showed increased glutamate *in vivo* after glutaminase inhibitor, CB-839 treatment is that tumors were able to use branch-chain fatty acid oxidation to replenish TCA cycle, and to further make glutamate. In order to examine whether fatty acids-derived carbon can contribute to glutamate and further glutamine synthesis, we will need to perform the ^{13}C-palmitate tracing experiment to identify the role of fatty acid oxidation.

KEGG pathways	***P-Value***
VALINE_LEUCINE_AND_ISOLEUCINE_DEGRADATION	0
DRUG_METABOLISM_OTHER_ENZYMES	0
RETINOL_METABOLISM	0
GLYCOLYSIS_GLUCONEOGENESIS	0
BUTANOATE_METABOLISM	0
METABOLISM_CYTOCHROME_P450	0.00203252
FATTY_ACID_METABOLISM	0
PENTOSE_AND_GLUCURONATE_INTERCONVERSIONS	0
ASCORBATE_AND_ALDARATE_METABOLISM	0.00403226
ABC_TRANSPORTERS	0.00202429
HOMOLOGOUS_RECOMBINATION	0.00592885
BASE_EXCISION_REPAIR	0.01434426
METABOLISM_OF_XENOBIOTICS_BY_CYTOCHROME_P450	0.00206186
PROPANOATE_METABOLISM	0.00998004
HISTIDINE_METABOLISM	0
PYRUVATE_METABOLISM	0
ARACHIDONIC_ACID_METABOLISM	0
P53_SIGNALING_PATHWAY	0
DNA_REPLICATION	0.032
PRIMARY_BILE_ACID_BIOSYNTHESIS	0.02296451
PEROXISOME	0.00210084
BETA_ALANINE_METABOLISM	0.01209677
ALLOGRAFT_REJECTION	0.01821862
MISMATCH_REPAIR	0.07692308
PYRIMIDINE_METABOLISM	0.02750491
PENTOSE_PHOSPHATE_PATHWAY	0.01825558
FC_GAMMA_R_MEDIATED_PHAGOCYTOSIS	0.0020284
ALZHEIMERS_DISEASE	0.02952756
ARRHYTHMOGENIC_RIGHT_VENTRICULAR_CARDIOMYOPATHY_ARVC	0
PURINE_METABOLISM	0.00982318

Figure 3.7. Top 30 significantly enriched pathways among genes upregulated in adapted clones combining with SUIT-2 and 8988T cells.

The intersection of gene expression in A-C (SUIT-2 and 8988T) that were significant and upregulated in comparison to NA-C were further subjected to pathways enrichment analysis by Gene Set Enrichment Analysis (GESA) software. FDR q-value of the cutoff is < 0.066. Bold indicates the pathways that I have discussed in the context.

a

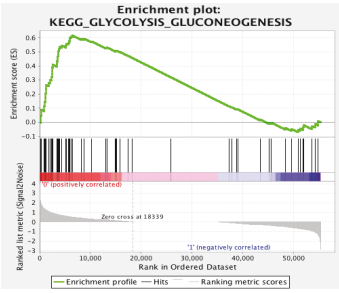
Enrichment plot:
KEGG_GLYCOLYSIS_GLUCONEOGENESIS
Enrichment score (ES)
Ranked list metric (Signal2Noise)
'0' (positively correlated)
Zero cross at 18339
'1' (negatively correlated)
Rank in Ordered Dataset
Enrichment profile
Hits
Ranking metric scores

b

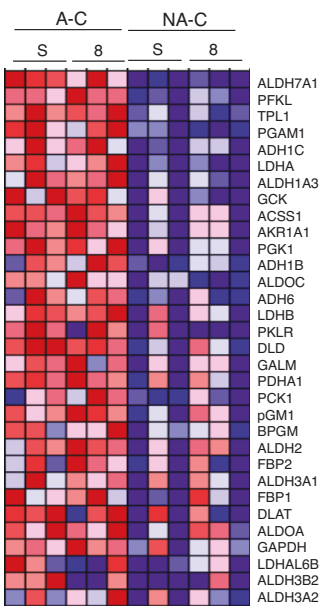
A-C
NA-C
S
8
S
8
ALDH7A1
PFKL
TPL1
PGAM1
ADH1C
LDHA
ALDH1A3
GCK
ACSS1
AKR1A1
PGK1
ADH1B
ALDOC
ADH6
LDHB
PKLR
DLD
GALM
PDHA1
PCK1
pGM1
BPGM
ALDH2
FBP2
ALDH3A1
FBP1
DLAT
ALDOA
GAPDH
LDHAL6B
ALDH3B2
ALDH3A2

c

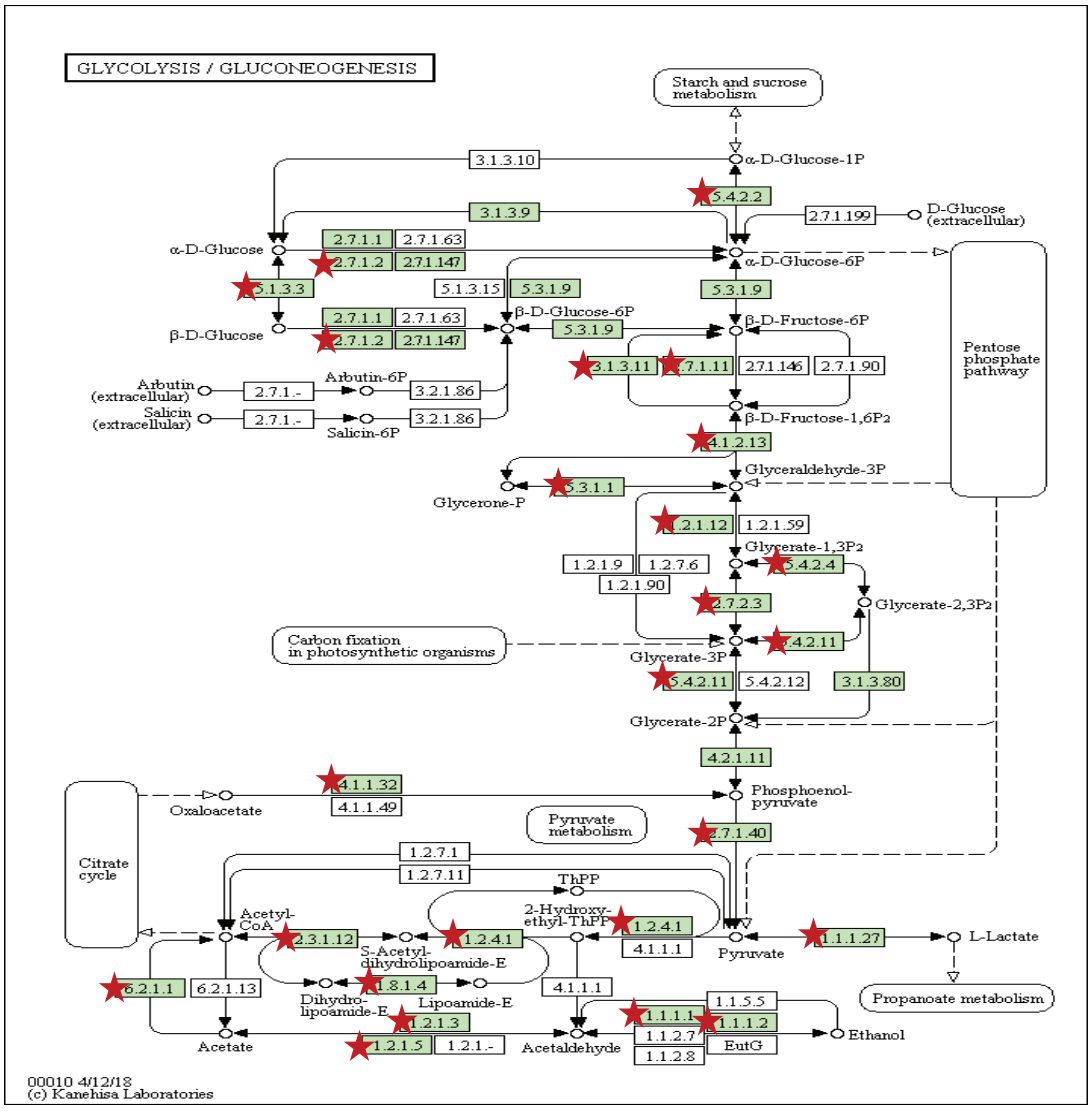
GLYCOLYSIS / GLUCONEOGENESIS
Starch and sucrose metabolism
α-D-Glucose-1P
D-Glucose (extracellular)
α-D-Glucose
α-D-Glucose-6P
β-D-Glucose
β-D-Glucose-6P
β-D-Fructose-6P
Pentose phosphate pathway
Arbutin (extracellular)
Arbutin-6P
Salicin (extracellular)
Salicin-6P
β-D-Fructose-1,6P2
Glyceraldehyde-3P
Glycerone-P
Glycerate-1,3P2
Glycerate-2,3P2
Carbon fixation in photosynthetic organisms
Glycerate-3P
Glycerate-2P
Phosphoenol-pyruvate
Oxaloacetate
Pyruvate metabolism
Citrate cycle
ThPP
2-Hydroxy-ethyl-ThPP
Acetyl-CoA
S-Acetyl-dihydrolipoamide-E
Pyruvate
L-Lactate
Propanoate metabolism
Dihydro-lipoamide-E
Lipoamide-E
Acetate
Acetaldehyde
Ethanol
00010 4/12/18
(c) Kanehisa Laboratories

Figure 3.8 (Continued)

The heatmap and a pathway illustration of genes upregulated in adapted clones within glycolysis/gluconeogenesis pathway compared to non-adapted clones under L-L conditions.

a, Gene enrichment plot that derived from GESA. **b**, Heatmaps of genes enriched and upregulated in A-C compared to NA-C under L-L conditions for 24 hours. **c**, Illustration of glycolysis/gluconeogenesis pathway. Red star indicates the expression is upregulated in A-C as shown in **b**. S refers to SUIT-2 cells; 8 refers to 8988T cells.

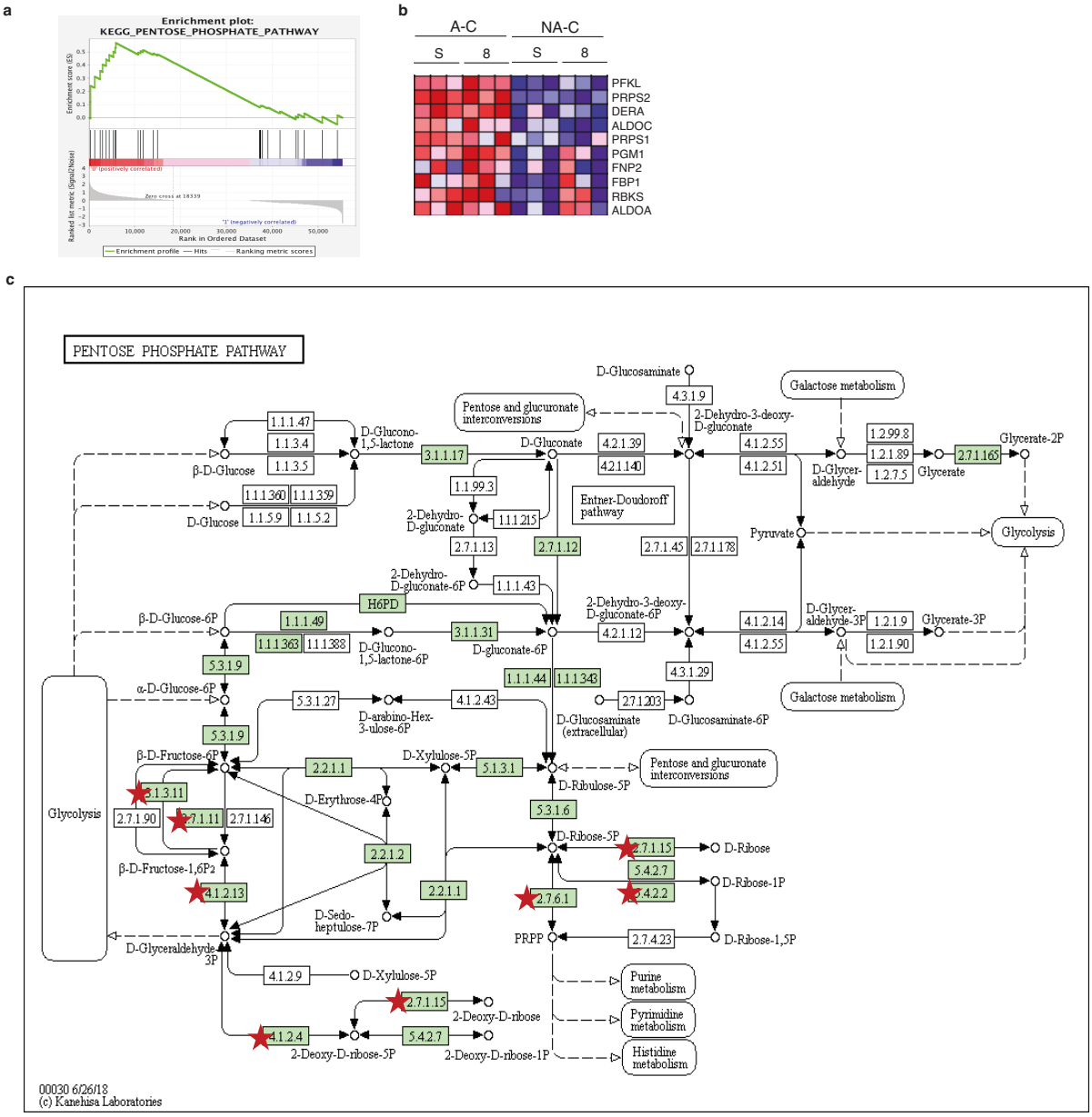

Figure. 3.9 The heatmap and a pathway illustration of genes upregulated in adapted clones within pentose phosphate pathway compared to non-adapted clones under L-L conditions. **a**, Gene enrichment plot that derived from GESA. **b**, Heatmaps of genes enriched and upregulated in A-C compared to NA-C under L-L conditions for 24 hours. **c**, Illustration of

Figure 3.9 (Continued)

pentose phosphate pathway. Red star indicates the expression is upregulated in A-C as shown in **b**. S refers to SUIT-2 cells; 8 refers to 8988T cells.

a

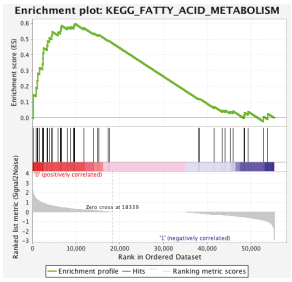
Enrichment plot: KEGG_FATTY_ACID_METABOLISM
Enrichment score (ES)
Ranked list metric (Signal2Noise)
'1' (positively correlated)
Zero cross at 18319
'-1' (negatively correlated)
Rank in Ordered Dataset
Enrichment profile
Hits
Ranking metric scores

b

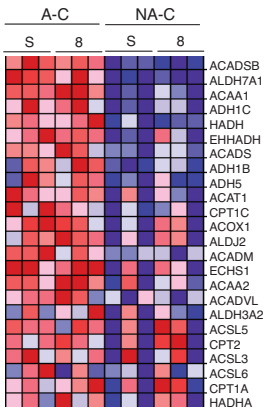
A-C
NA-C
S
8
S
8
ACADSB
ALDH7A1
ACAA1
ADH1C
HADH
EHHADH
ACADS
ADH1B
ADH5
ACAT1
CPT1C
ACOX1
ALDJ2
ACADM
ECHS1
ACAA2
ACADVL
ALDH3A2
ACSL5
CPT2
ACSL3
ACSL6
CPT1A
HADHA

c

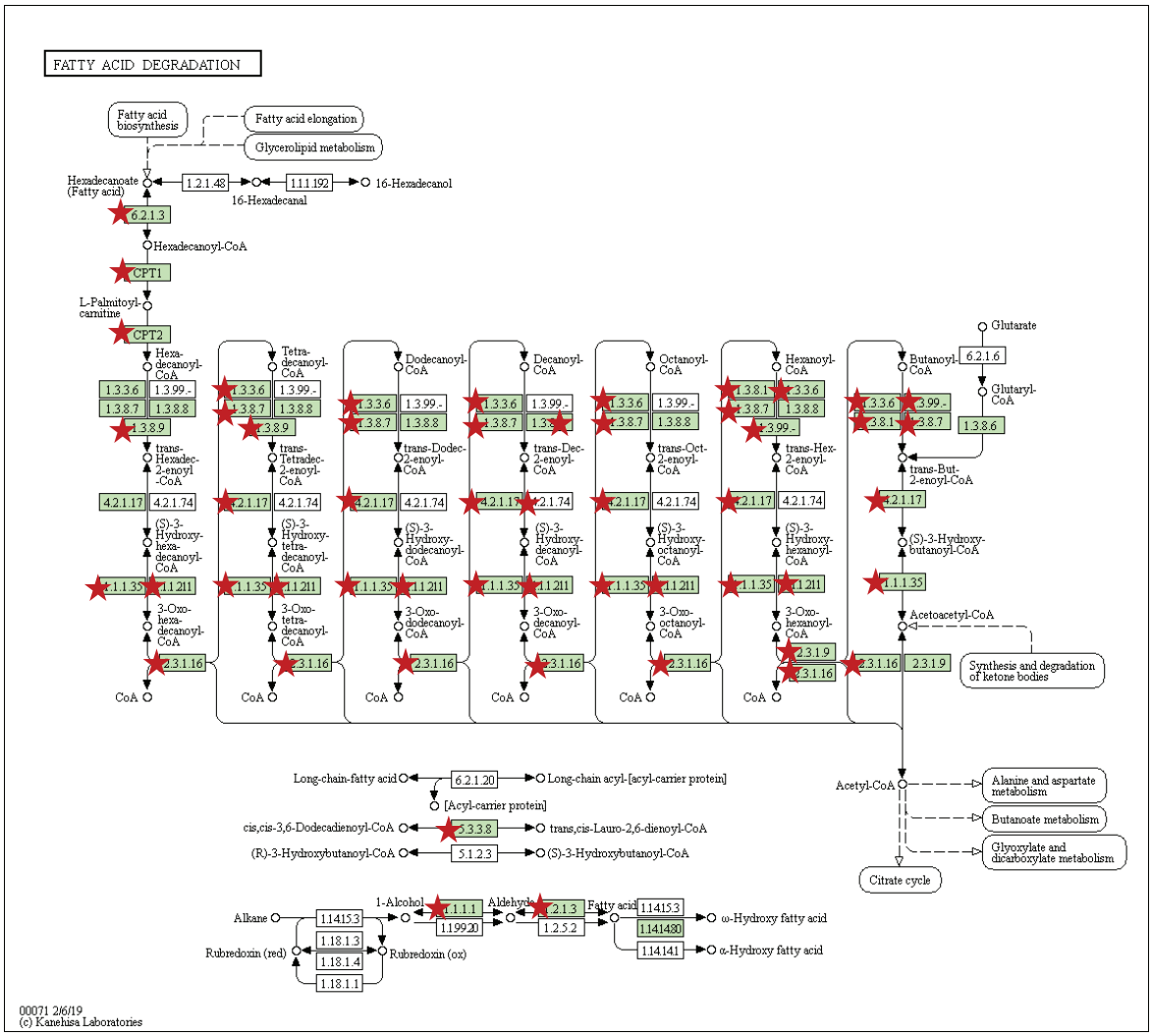
FATTY ACID DEGRADATION
Fatty acid biosynthesis
Fatty acid elongation
Glycerolipid metabolism
Hexadecanoate (Fatty acid)
1.2.1.48
16-Hexadecanal
1.1.1.192
16-Hexadecanol
6.2.1.3
Hexadecanoyl-CoA
CPT1
L-Palmitoyl-carnitine
CPT2
Hexadecanoyl-CoA
Tetradecanoyl-CoA
Dodecanoyl-CoA
Decanoyl-CoA
Octanoyl-CoA
Hexanoyl-CoA
Butanoyl-CoA
Glutarate
Glutaryl-CoA
6.2.1.6
1.3.8.6
trans-Hexadec-2-enoyl-CoA
trans-Tetradec-2-enoyl-CoA
trans-Dodec-2-enoyl-CoA
trans-Dec-2-enoyl-CoA
trans-Oct-2-enoyl-CoA
trans-Hex-2-enoyl-CoA
trans-But-2-enoyl-CoA
4.2.1.17
4.2.1.74
(S)-3-Hydroxy-hexadecanoyl-CoA
(S)-3-Hydroxy-tetradecanoyl-CoA
(S)-3-Hydroxy-dodecanoyl-CoA
(S)-3-Hydroxy-decanoyl-CoA
(S)-3-Hydroxy-octanoyl-CoA
(S)-3-Hydroxy-hexanoyl-CoA
(S)-3-Hydroxy-butanoyl-CoA
1.1.1.35
1.1.211
3-Oxo-hexadecanoyl-CoA
3-Oxo-tetradecanoyl-CoA
3-Oxo-dodecanoyl-CoA
3-Oxo-decanoyl-CoA
3-Oxo-octanoyl-CoA
3-Oxo-hexanoyl-CoA
Acetoacetyl-CoA
2.3.1.16
2.3.1.9
CoA
Synthesis and degradation of ketone bodies
Long-chain-fatty acid
6.2.1.20
Long-chain acyl-[acyl-carrier protein]
[Acyl-carrier protein]
cis,cis-3,6-Dodecadienoyl-CoA
5.3.3.8
trans,cis-Lauro-2,6-dienoyl-CoA
(R)-3-Hydroxybutanoyl-CoA
5.1.2.3
(S)-3-Hydroxybutanoyl-CoA
Acetyl-CoA
Alanine and aspartate metabolism
Butanoate metabolism
Glyoxylate and dicarboxylate metabolism
Citrate cycle
Alkane
1.14.15.3
1-Alcohol
1.1.1.1
1.1.99.20
Aldehyde
1.2.1.3
1.2.5.2
Fatty acid
1.14.15.3
1.14.14.80
1.14.14.1
ω-Hydroxy fatty acid
α-Hydroxy fatty acid
Rubredoxin (red)
1.18.1.3
1.18.1.4
1.18.1.1
Rubredoxin (ox)
00071 2/6/19
(c) Kanehisa Laboratories

Figure 3.10 (Continued)

The heatmap and a pathway illustration of genes upregulated in adapted clones within fatty acid degradation pathway compared to non-adapted clones under L-L conditions.

a, Gene enrichment plot that derived from GESA. **b**, Heatmaps of genes enriched and upregulated in A-C compared to NA-C under L-L conditions for 24 hours. **c**, Illustration of fatty acid degradation pathway. Red star indicates the expression is upregulated in A-C as shown in **b**. S refers to SUIT-2 cells; 8 refers to 8988T cells.

3.7 How to apply the reliance of glutamine synthesis in PDAC as an intervention in pre-clinical experiments?

Several reports demonstrated that cancer cells express GS under a glutamine-starved condition with the implication that GS could be a potential target given that tumors might reside in a nutrient-harsh environment *in vivo*. One recent report showed that either treating tumor-bearing mice with a pharmacological intervention of a selective irreversible inhibitor of GS, Methionine sulfoximine (MSO), or genetically manipulating glutamine synthesis through silencing GLUL (the gene name of GS), resulted in a reduction of tumor growth in sarcoma (*13*). It will be important to test whether MSO treatment or inhibition of GS by genetic approaches can also affect PDAC tumor growth or prolong survival in *vivo*.

3.8 Conclusions

This dissertation demonstrates an adapted mechanism in pancreatic cancer under a glucose- and glutamine-deprived conditions, which might occur *in vivo* microenvironment. My work has demonstrated the importance of glutamine synthesis activity that is elevated in the cells surviving under prolonged nutrient starvation conditions by utilizing other amino acids sources. In addition, we revealed another role of mTORC1 signaling, which can stabilize glutamine synthetase protein and further help PDAC cells re-synthesize glutamine under these circumstances. Together with my current findings and future work, we will potentially reveal a potential target to treat this deadly cancer.

3.9 Reference

1. J. Kim, K.-L. Guan, mTOR as a central hub of nutrient signalling and cell growth. *Nature cell biology* **21**, 63 (2019).

2. V. S. Rodrik-Outmezguine *et al.*, mTOR kinase inhibition causes feedback-dependent biphasic regulation of AKT signaling. *Cancer discovery* **1**, 248-259 (2011).

3. A. J. Bott *et al.*, Oncogenic Myc induces expression of glutamine synthetase through promoter demethylation. *Cell metabolism* **22**, 1068-1077 (2015).

4. S. Tardito *et al.*, Glutamine synthetase activity fuels nucleotide biosynthesis and supports growth of glutamine-restricted glioblastoma. *Nature cell biology* **17**, 1556 (2015).

5. M. Tajan *et al.*, A role for p53 in the adaptation to glutamine starvation through the expression of SLC1A3. *Cell metabolism* **28**, 721-736. e726 (2018).

6. T. V. Nguyen *et al.*, Glutamine Triggers Acetylation-Dependent Degradation of Glutamine Synthetase via the Thalidomide Receptor Cereblon. *Mol Cell* **61**, 809-820 (2016).

7. M. Pan *et al.*, Regional glutamine deficiency in tumours promotes dedifferentiation through inhibition of histone demethylation. *Nature cell biology* **18**, 1090 (2016).

8. L. Yang *et al.*, Targeting stromal glutamine synthetase in tumors disrupts tumor microenvironment-regulated cancer cell growth. *Cell metabolism* **24**, 685-700 (2016).

9. P. P. Hsu *et al.*, The mTOR-regulated phosphoproteome reveals a mechanism of mTORC1-mediated inhibition of growth factor signaling. *Science* **332**, 1317-1322 (2011).

10. J. Zhao, B. Zhai, S. P. Gygi, A. L. Goldberg, mTOR inhibition activates overall protein degradation by the ubiquitin proteasome system as well as by autophagy. *Proceedings of the National Academy of Sciences* **112**, 15790-15797 (2015).

11. N. N. Pavlova *et al.*, As extracellular glutamine levels decline, asparagine becomes an essential amino acid. *Cell metabolism* **27**, 428-438. e425 (2018).

12. D. E. Biancur *et al.*, Compensatory metabolic networks in pancreatic cancers upon perturbation of glutamine metabolism. *Nature communications* **8**, 15965 (2017).

13. S. H. Issaq, A. Mendoza, S. D. Fox, L. J. Helman, Glutamine synthetase is necessary for sarcoma adaptation to glutamine deprivation and tumor growth. *Oncogenesis* **8**, 20 (2019).